

Transfer Learning through Enhanced Sufficient Representation: Enriching Source Domain Knowledge with Target Data

Yeheng Ge^{a,*}, Xueyu Zhou^{a,*}, and Jian Huang^{a,b,†}

^aDepartment of Data Science and Artificial Intelligence, The Hong Kong Polytechnic University

^bDepartment of Applied Mathematics, The Hong Kong Polytechnic University

March 3, 2025

Abstract

Transfer learning is an important approach for addressing the challenges posed by limited data availability in various applications. It accomplishes this by transferring knowledge from well-established source domains to a less familiar target domain. However, traditional transfer learning methods often face difficulties due to rigid model assumptions and the need for a high degree of similarity between source and target domain models. In this paper, we introduce a novel method for transfer learning called Transfer learning through Enhanced Sufficient Representation (TESR). Our approach begins by estimating a sufficient and invariant representation from the source domains. This representation is then enhanced with an independent component derived from the target data, ensuring that it is sufficient for the target domain and adaptable to its specific characteristics. A notable advantage of TESR is that it does not rely on assuming similar model structures across different tasks. For example, the source domain models can be regression models, while the target domain task can be classification. This flexibility makes TESR applicable to a wide range of supervised learning problems. We explore the theoretical properties of TESR and validate its performance through simulation studies and real-world data applications, demonstrating its effectiveness in finite sample settings.

Keywords: Conditional independence; Domain heterogeneity; Invariant representation; Representation enhancement; Supervised learning.

*Equal contributions

†Corresponding author

1 Introduction

Transfer learning has emerged as a powerful paradigm in statistics and machine learning, enabling models to leverage knowledge from related tasks to enhance performance on a target task with limited data (Pan and Yang, 2009; Torrey and Shavlik, 2010). Traditional machine learning approaches often require large amounts of data, which can be costly and time-consuming to obtain. Transfer learning addresses the data scarcity problem by transferring knowledge from source domains, where data is abundant, to a target domain, where data is scarce (Weiss et al., 2016). Despite its success, existing transfer learning methods often face limitations in terms of scalability and adaptability to diverse domains (Zhuang et al., 2020). In this paper, we propose a novel transfer learning method that overcomes these limitations by introducing a more flexible framework. This framework is capable of efficiently adapting to various target domains while maintaining high performance. Our approach builds upon recent advancements in sufficient representation learning and invariant risk minimization, offering a robust solution to the challenges faced by current transfer learning methodologies.

The interest in transfer learning across various settings has grown significantly in recent years. Many existing studies have focused on developing transfer learning methods and theories within parametric modeling frameworks. For instance, Bastani (2021) investigates transfer learning in high-dimensional linear regression with a large source dataset, providing an upper bound for the estimation error. Similarly, Li et al. (2022) propose a transfer learning method with mini-max optimality in high-dimensional sparse linear regression, featuring a data-driven algorithm to exclude dissimilar source datasets. Both studies assume a small difference between the regression functions of the source and target domains as a prerequisite for successful knowledge transfer. Additionally, Gu et al. (2024) introduce angle-based similarity for transfer learning in high-dimensional linear models. In the context of non-parametric models, Cai and Wei (2021) explore transfer learning for non-parametric classification, defining similarity through the relative signal exponent of the regression function. Cai and Pu (2022) examine transfer learning in non-parametric regression models.

These studies require that the models used for both the source and target domains share the same functional form, with similar model parameters across these domains. Knowledge transfer is achieved by transferring parameter estimates from the source domains to the target domain. However, the assumption of having the same model form across domains can be restrictive and may not hold in many real-world scenarios. For example, the source domain might involve a classification problem for cancer sub-types, while the target domain focuses on prognosis prediction for the same cancer. Transferring information from the classification outcomes to a continuous prognosis prediction task presents significant challenges. This limitation highlights the need for more flexible and robust transfer learning approaches that can accommodate varying model forms and complex relationships between domains.

It has been suggested that features with strong predictive power offer a significant advantage in transfer learning (Bengio et al., 2013; Neyshabur et al., 2020). Building on this idea, some existing works on transfer learning assume that all tasks share a common representation (Maurer et al., 2016; Arjovsky et al., 2019; Hu et al., 2022). Under this shared representation assumption, features learned from the source data can be directly applied to the target task, facilitating efficient knowledge transfer. However, in practice, representations from related tasks are often similar but not identical (Cai and Wei, 2021). Beyond the condition of shared representations, it is important to investigate the role of sufficient representations in facilitating knowledge trans-

fer for general supervised learning problems. Recently, several authors have developed nonlinear representation learning methods based on sufficient dimension reduction (Lee et al., 2013; Huang et al., 2024; Chen et al., 2024). Jiao et al. (2024) consider transferring source domain sufficient and domain-invariant representations to the target task. They develop the prediction model for the target task, assuming a linear relationship between the transferred source domain representations and the response of interest. Despite these advancements, the study of data representations in transfer learning problems remains under-explored. Specifically, it remains unclear how to construct representations that can leverage knowledge from source domains while simultaneously capturing specific information from the target domain for general supervised learning problems.

In this paper, we introduce a novel transfer learning method that facilitates knowledge transfer through data representation. Specifically, the proposed method first estimates a sufficient and invariant representation from the source domains. This representation is then enhanced with additional independent representations obtained from the target data, which allow us to adapt to the specific characteristics of the target domain. This enhancement strategy ensures its sufficiency for the target domain and still leverages valuable information from the source domains. For simplicity, we refer to the proposed method as Transfer learning through Enhanced Sufficient Representation (TESR).

A notable advantage of TESR is that it does not rely on assuming similar model structures across different tasks. For example, the source domain models can be regression models, while the target domain task can be classification. This flexibility makes TESR applicable to a wide range of supervised learning problems where the source and target domains may differ substantially. Additionally, unlike conventional transfer learning approaches, which typically transfer model parameters, a key feature of TESR is that it focuses on transferring data representations from sources to the target domain. Another important aspect of TESR is that it does not assume that a representation sufficient for the source domain will also be sufficient for the target domain. Instead, we posit that a sufficient representation in the source domains provides useful information for the target domain. This assumption allows for greater flexibility and adaptability in the transfer learning.

This paper is structured as follows: Section 2 presents the framework of the proposed TESR method. It presents the underlying principles and architecture of TESR. In Section 3, we describe the objective functions for TESR and outlines the estimation procedure. Section 4 establishes the convergence rate of the proposed method and examines its theoretical advantages. Section 5 evaluates the numerical performance of TESR through a series of simulation studies. Additionally, Section 6 illustrates the method’s practical applications by applying it to two real-world datasets. Finally, Section 7 discusses the findings and suggests potential directions for future research.

2 Method

In this section, we present the framework of Transfer Learning through Sufficient and Invariant Representation. We begin by learning a sufficient and invariant representation (SIRep) from the source data. Next, we enhance SIRep with an augmented component derived from the target data. This augmented component is specifically designed to capture information present in the target dataset that is not contained in the SIRep.

Suppose that there are $S + 1$ domains denoted as $\mathcal{D}_s = \{X_s, Y_s\}$ for $s = 0, 1, \dots, S$, where $X_s \in \mathbb{R}^d$ is the vector of predictors and $Y_s \in \mathbb{R}^{q_s}$ is the vector of responses for task s . We denote

$s = 0$ as the index of the target domain and $s = 1, \dots, S$ as the source domains. Let $n_s = |\mathcal{D}_s|$ be the sample size of the s th domain. We are mainly interested in the scenario when the sample size of the target dataset $n_0 = |\mathcal{D}_0|$ is limited, and the total sample size of the source datasets $N = \sum_{s=1}^S n_s$ is large.

The goal of transfer learning is to improve performance on the target task by leveraging information from source datasets. In this work, we allow the possibility that the source datasets may not share the same structure as the target dataset. For instance, the source domain task might involve a regression problem, whereas the target domain task could involve a classification problem.

2.1 Sufficient representation

For a given domain s , a sufficient representation is a measurable function $R_s : \mathbb{R}^d \rightarrow \mathbb{R}^{r_s}$ with the property (Huang et al., 2024):

$$Y_s \perp\!\!\!\perp X_s \mid R_s(X_s), \quad s = 0, 1, \dots, S, \quad (1)$$

that is, Y_s and X_s are conditionally independent given $R_s(X_s)$. This implies the representation $R_s(X_s)$ contains all the information in X_s relevant to Y_s . This formulation is a nonparametric generalization of the basic condition in sufficient dimension reduction (Li, 1991; Cook and Ni, 2005), where it is assumed $R_s(X_s) = B_s^T X_s$ with $B_s \in \mathbb{R}^{d \times r_s}$ satisfying $B_s^T B_s = I_{r_s}$. We refer to Huang et al. (2024) and Chen et al. (2024) for discussions on nonlinear sufficient representation.

2.2 Sufficient and invariant representation of source data

The main challenge in transfer learning lies in determining the specific type of knowledge that should be transferred from the source domains to the target domain. We want to transfer the most essential and relevant knowledge from these source domains to enhance the performance in the target domain. One effective approach to identifying this essential knowledge is through the concept of invariance (Arjovsky et al., 2019; Jiao et al., 2024). Invariance refers to the consistent and stable knowledge encoded in the predictors. Therefore, invariant representations from the source domains are expected to carry the most essential and robust knowledge, thus enjoying high generalization power to unknown target domain.

Therefore, we consider a common representation $R_c(\cdot)$ that is sufficient and invariant for all the source domains. We denote the joint dataset where the sources $s = 1, \dots, S$ are pooled together as $\mathcal{D}_{pool} = \{X_{pool}, Y_{pool}, Z\}$, where $Z \in \{1, \dots, S\}$ is the categorical indicator as the index of the domains. The pooled dataset \mathcal{D}_{pool} is of sample size $N = \sum_{s=1}^S n_s$ and $Z_i = s$ means the sample point $(X_{pool,i}, Y_{pool,i})$ is from the dataset \mathcal{D}_s . Then a sufficient and invariant representation (SIRep) for the source domains is defined as a function R_c that satisfies

$$Y_s \perp\!\!\!\perp X_s \mid R_c(X_s) \quad \text{and} \quad R_c(X_{pool}) \perp\!\!\!\perp Z, \quad \text{for } s = 1, \dots, S. \quad (2)$$

The first term $Y_s \perp\!\!\!\perp X_s \mid R_c(X_s)$ implies that $R_c(\cdot)$ is sufficient for all the source domains. The second term $R_c(X_{pool}) \perp\!\!\!\perp Z$ implies that the distributions of $R_c(X_s)$ are unchanged across the sources $s = 1, \dots, S$. These invariant features are essential to ensure the transferred knowledge is both robust and applicable to new target domains (Arjovsky et al., 2019; Jiao et al., 2024). Such a representation always exists, since a trivial solution is $R_c = [R_1, \dots, R_S]$ that concatenates all

the sufficient representations from the sources. Of course, such a simple combination of the individual sufficient representations is generally not an efficient solution for invariant representation as the R_s for $s = 1, \dots, S$ may share some information, leading to overlapping components in terms of information content in the concatenated representation.

The estimation of sufficient and invariant representations does not preclude the existence of heterogeneity among the source domains. As mentioned earlier, in the extreme case where all source domains have different sufficient representations, we can simply concatenate these distinct representations. Generally, greater heterogeneity may result in a more complex invariant representation, while less heterogeneity leads to simpler ones. In practice, the extent of heterogeneity among source domains is often unknown. The proposed invariant representation method does not require prior knowledge of this heterogeneity or identification of which sources differ.

2.3 Enhancing source domain representation with target data

A critical issue is that a representation that is sufficient for the source domains may not be sufficient for the target domain. This discrepancy arises due to potential differences between the data distributions of the source and target domains. Consequently, it is essential to enhance the SIRep from the sources using the target data.

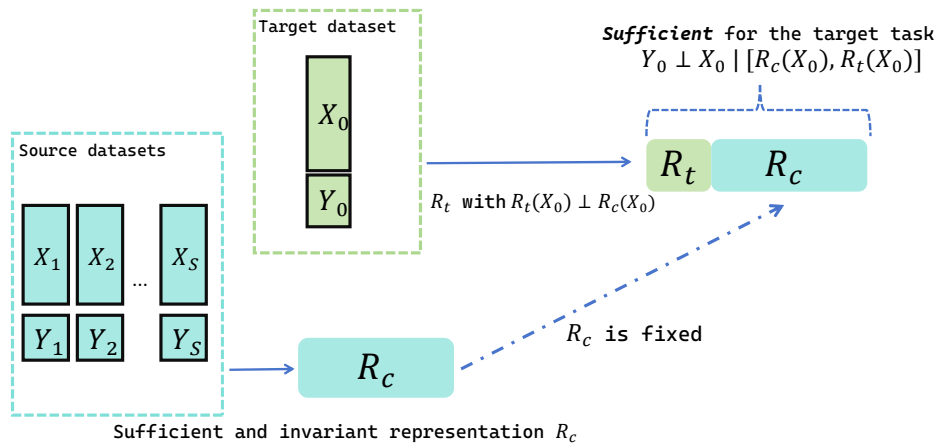


Figure 1: The illustration of the proposed framework. The sufficient and invariant representation R_c summarizes information from the sources, while R_t captures specific information relevant to the target task, ensuring that $[R_c, R_t]$ is sufficient for the target data. Importantly, $R_t(X_0)$ and $R_c(X_0)$ are required to be independent.

We enrich the source data representation R_c with an additional component R_t such that the combined representation $[R_c, R_t]$ satisfies the following two requirements:

- The combined representation is sufficient for the target data, that is,

$$Y_0 \perp\!\!\!\perp X_0 \mid [R_c(X_0), R_t(X_0)]. \quad (3)$$

- Any additional information represented by R_t for the target data, if necessary, should be independent of R_c , that is,

$$R_c(X_0) \perp\!\!\!\perp R_t(X_0). \quad (4)$$

Condition (3) ensures that the target response Y_0 is independent of the target predictors X_0 given the combined representation $[R_c(X_0), R_t(X_0)]$. By achieving this, we can effectively leverage the knowledge from the source domains while adapting to the specific characteristics of the target domain. Meanwhile, by requiring the independence condition (4), we avoid learning information that already captured by R_c with limited target dataset. Figure 1 illustrates our framework.

The existence of R_t is always guaranteed, since for any given R_c , we can set $R_t = R_0$, the sufficient representation for target domain, ignoring the contribution of R_c . Generally, R_t can be significantly simpler and easier to estimate than R_0 , when R_c already contains a significant amount of the information for a sufficient representation in the \mathcal{D}_0 . This representation learning approach aligns with the rationale of transfer learning, which seeks to leverage transferred knowledge to reduce the modeling complexity. By decomposing the representation into R_c and R_t , we can isolate the complex, invariant features captured by R_c from the simpler, target-specific features captured by R_t .

By enhancing the source data representation with a component learned from the target data, we aim to create a combined representation that is both sufficient and adaptable. This dual-focus strategy allows us to effectively utilize the valuable knowledge from the source domains while tailoring the model to address the unique characteristics of the target domain. This results in a more robust, accurate, and generalizable model that can better achieve the overarching goals of transfer learning.

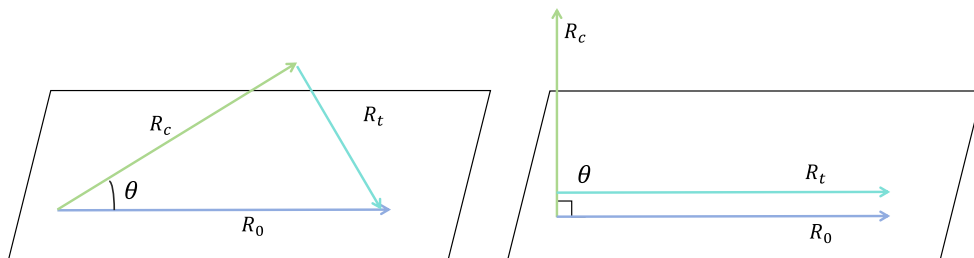


Figure 2: The relationships between R_c , R_t , and R_0 . Estimating R_t is simpler than estimating R_0 when $R_c \not\perp R_0$ (left panel) with dataset \mathcal{D}_0 because R_c contains useful information about R_0 . Conversely, when source data does not contain useful information about the target data, meaning $R_c \perp R_0$ (right panel), estimating R_t is similar to directly estimating R_0 .

Figure 2 illustrates how TESR adapts to the heterogeneity between source and target data. In cases where R_c provides useful information about R_0 (left panel), R_t can be learned such that the combination $[R_c, R_t]$ captures all the information necessary to recover R_0 . Conversely, if R_c is irrelevant or uninformative (right panel), that is, the source domains do not contain any useful information about the target domain, then we have $R_t = R_0$. This adaptability makes TESR robust to both the presence and absence of meaningful information in R_c for the target task. Additionally, the property $R_t \perp\!\!\!\perp R_c$ ensures that the target dataset is used exclusively to

learn new information that cannot be obtained from the source datasets, leading to the efficient use of the limited sample size available in the target dataset.

3 Estimation method

We implement the TESR framework in two steps: First, we estimate R_c using all source datasets \mathcal{D}_s with $s = 1, \dots, S$. Then, with the estimated R_c , we estimate R_t on the target task \mathcal{D}_0 , ensuring orthogonality between $R_c(X_0)$ and $R_t(X_0)$. The combined representation $[R_c, R_t]$ is then used for the target task on \mathcal{D}_0 .

3.1 Preliminaries

In this subsection, we describe the measures that will be used for characterizing independence and equality in distributions.

3.1.1 Distance covariance

Let \mathbb{V} be a dependence measure between random variables U and V with the following properties: (a) $\mathbb{V}[U, V] \geq 0$ with $\mathbb{V}[U, V] = 0$ if and only if $U \perp V$; (b) $\mathbb{V}[U, V] \geq \mathbb{V}[R(U), V]$ for every measurable function R ; (c) $\mathbb{V}[U, V] = \mathbb{V}[R^*(U), V]$ if and only if R^* is sufficient. These properties imply that R^* is a sufficient representation for prediction V if and only if $R^* \in \operatorname{argmin}_R \{-\mathbb{V}[R(U), V]\}$.

We use distance covariance to measure the dependence of two random variables (Székely et al., 2007). Let i be the imaginary unit $(-1)^{1/2}$. For any $\mathbf{s} \in \mathbb{R}^d$ and $\mathbf{t} \in \mathbb{R}^m$, let $\psi_U(\mathbf{s}) = \mathbb{E}[\exp^{i\mathbf{s}^T U}]$, $\psi_V(\mathbf{t}) = \mathbb{E}[\exp^{i\mathbf{t}^T V}]$, and $\psi_{U,V}(\mathbf{s}, \mathbf{t}) = \mathbb{E}[\exp^{i(\mathbf{s}^T U + \mathbf{t}^T V)}]$ be the characteristic functions of random vectors $U \in \mathbb{R}^d$, $V \in \mathbb{R}^m$, and the pair (U, V) , respectively. A specific squared distance covariance $\mathbb{V}[U, V]$ is defined as

$$\mathbb{V}[U, V] = \int_{\mathbb{R}^{d+m}} \frac{|\psi_{U,V}(\mathbf{s}, \mathbf{t}) - \psi_U(\mathbf{s})\psi_V(\mathbf{t})|^2}{c_d c_m \|\mathbf{s}\|^{d+1} \|\mathbf{t}\|^{m+1}} d\mathbf{s} d\mathbf{t},$$

where $c_d = \frac{\pi^{(d+1)/2}}{\Gamma((d+1)/2)}$. This form of distance covariance has a simple expression,

$$\begin{aligned} \mathbb{V}(U, V) = & \mathbb{E}\|U - U'\|\|V - V'\| + \mathbb{E}\|U - U'\|\mathbb{E}\|V - V'\| \\ & - \mathbb{E}\|U - U'\|\|V - V''\| - \mathbb{E}\|U - U''\|\|V - V'\|, \end{aligned}$$

where $\|\cdot\|$ is the Euclidean distance, $\{U', V'\}$ and $\{U'', V''\}$ are independent copies of (U, V) .

Given n i.i.d. copies $\{U_i, V_i\}_{i=1}^n$ of (U, V) , an unbiased estimator of \mathbb{V} is the empirical distance covariance $\widehat{\mathbb{V}}_n$, which can be elegantly expressed as a U -statistic (Huo and Székely, 2016)

$$\widehat{\mathbb{V}}_n[U, V] = \frac{1}{\binom{n}{4}} \sum_{1 \leq i_1 < i_2 < i_3 < i_4 \leq n} h((U_{i_1}, V_{i_1}), \dots, (U_{i_4}, V_{i_4})),$$

where h is the kernel defined by

$$\begin{aligned}
 h((u_1, v_1), \dots, (u_4, v_4)) &= \frac{1}{4} \sum_{\substack{1 \leq i, j \leq 4 \\ i \neq j}} \|u_i - u_j\| \|v_i - v_j\| + \frac{1}{24} \sum_{\substack{1 \leq i, j \leq 4 \\ i \neq j}} \|u_i - u_j\| \sum_{\substack{1 \leq i, j \leq 4 \\ i \neq j}} \|v_i - v_j\| \\
 &\quad - \frac{1}{4} \sum_{i=1}^4 \left(\sum_{\substack{1 \leq j \leq 4 \\ j \neq i}} \|u_i - u_j\| \sum_{\substack{1 \leq j \leq 4 \\ i \neq j}} \|v_i - v_j\| \right).
 \end{aligned}$$

3.1.2 Energy distance

Since sufficiency is invariant under one-to-one transformations, it is always possible to transform a sufficient representation $R^*(X)$ to have a Gaussian distribution, under the assumption that $R^*(X)$ has a finite second moment and is absolutely continuous with respect to the Gaussian distribution (Huang et al., 2024). Therefore, we can restrict the space of sufficient representations to those with a standard Gaussian distribution. For the Gaussian regularization, we use a divergence measure \mathbb{D} to quantify the difference between the distributions of two random variables U and V . This measure should satisfy the condition $\mathbb{D}(U\|V) \geq 0$ and $\mathbb{D}(U\|V) = 0$ if and only if U and V have the same distribution. In this work, we use the energy distance (Rizzo and Székely, 2016),

$$\mathbb{D}(U\|V) = 2\mathbb{E}\|U - V\| - \mathbb{E}\|U - U'\| - \mathbb{E}\|V - V'\|, \quad (5)$$

where $\{U', V'\}$ are independent copies of $\{U, V\}$, respectively. We note that Huang et al. (2024) used Generative Adversarial Networks (GANs) to push the distribution of data representations to a Gaussian distribution. However, GAN-based regularization requires complex optimization designs and may lead to suboptimal convergence in practice. In contrast, the energy distance used is simpler and easier to compute, providing a practical alternative to GAN-based approaches.

When two empirical samples $\{U_i, i = 1, \dots, n\}$ and $\{V_j, j = 1, \dots, n\}$ are available, following the suggestion of Gretton et al. (2012), we use the following empirical version of the energy distance,

$$\mathbb{D}_n(U\|V) = \frac{1}{\binom{n}{2}} \sum_{1 \leq i, j \leq n} h_e(u_i, u_j; v_i, v_j), \quad (6)$$

where $h_e(u_1, u_2; v_1, v_2) = \|u_1 - v_2\| + \|u_2 - v_1\| - \|u_1 - u_2\| - \|v_1 - v_2\|$.

3.2 Estimating sufficient and invariance representation from source data

We first present the proposed method for estimating a SIRep R_c from the source datasets $\mathcal{D}_s, s = 1, \dots, S$. We are interested in estimating a representation characterized in (2). Based on (2), a SIRep R_c can be characterized as a solution to the constrained optimization problem:

$$\begin{aligned}
 R_c^* &= \operatorname{argmin}_R \left\{ - \sum_{s=1}^S \mathbb{V}(R(X_s), Y_s) \right\}, \\
 &\text{subject to } R(X_s) \sim N(0, \mathbf{I}) \text{ and } R(X_{pool}) \perp\!\!\!\perp Z, \text{ for } s = 1, \dots, S,
 \end{aligned} \quad (7)$$

where, as discussed in Subsection 3.1.2, we imposed a constraint that the representation has a Gaussian distribution. The Lagrangian form of (7) is

$$\mathcal{L}_S(R) = \sum_{s=1}^S \left\{ -\mathbb{V}(R(X_s), Y_s) + \lambda_E \mathbb{D}(R(X_s) \| \gamma_{r_c}) \right\} + \lambda_Z \mathbb{V}(R(X_{pool}), Z), \quad (8)$$

where $\gamma_{r_c} \sim N(0, \mathbf{I}_{r_c})$, λ_E and λ_Z are regularization parameters.

Now suppose we have source datasets $\mathcal{D}_s = \{X_{s,i}, Y_{s,i}, i = 1, \dots, n_s\}, s = 1, \dots, S$. Let $\mathbb{V}_n(\cdot, \cdot)$ be the empirical distance covariance defined in (5), and let $\mathbb{D}_n(\cdot \| \cdot)$ be the empirical version of the energy distance defined in (6). Then we have the empirical objective function,

$$\mathcal{L}_{S,n}(R) = \sum_{s=1}^S \left\{ -\mathbb{V}_n(R(X_s), Y_s) + \lambda_E \mathbb{D}_n(R(X_s) \| \gamma_{r_c}) \right\} + \lambda_Z \mathbb{V}_n(R(X_{pool}), Z), \quad (9)$$

where X_{pool} is the pooled covariates from $\mathcal{D}_s, s = 1, \dots, S$, Z is the one-hot domain indicator, λ_E and λ_Z are tuning parameters. Then $\widehat{R}_c = \operatorname{argmin}_{R \in \mathcal{F}_{R_c}} \mathcal{L}_{S,n}(R)$.

3.3 Estimating enhanced representation with target data

After a SIRep R_c is derived from the source datasets is obtained, we move on to construct a representation for the target data. If there is no difference between the source and target data, we can simply use R_c as the representation for the target dataset. However, to account for potential heterogeneity between the source and target data, we enhance R_c using the target data.

Specifically, for a given R_c and the target data $\mathcal{D}_0 = \{X_0, Y_0\}$, we seek an augmentation R_t that satisfies (4). This can be equivalently formulated as an optimization problem with the objective

$$\begin{aligned} R_t^* &= \operatorname{argmin}_R \{ -\mathbb{V}([R(X_0), R_c(X_0)], Y_0) \}, \\ &\text{subject to } R(X_0) \perp R_c(X_0) \text{ and } R(X_0) \sim N(0, \mathbf{I}), \end{aligned} \quad (10)$$

where similar to Subsection 3.1.2, we require the augmentation R_t^* to be Gaussian.

We reformulate this problem by expressing the objective function in the Lagrangian form,

$$\mathcal{L}_T(R, R_c) = -\mathbb{V}([R(X_0), R_c(X_0)], Y_0) + \lambda_C \mathbb{V}(R(X_0), R_c(X_0)) + \lambda_{E,0} \mathbb{D}(R(X_0) \| \gamma_{r_t}), \quad (11)$$

where $\gamma_{r_t} \sim N(0, \mathbf{I}_{r_t})$, the $\lambda_C \geq 0$ and $\lambda_{E,0} \geq 0$ are regularization parameters. Then for a given estimator \widehat{R}_c based on the source datasets, we augment it by

$$\widehat{R}_t = \operatorname{argmin}_{R \in \mathcal{F}_{R_t}} \mathcal{L}_{T,n}([R, \widehat{R}_c]), \quad (12)$$

with $\mathcal{L}_{T,n}(R, \widehat{R}_c) = -\mathbb{V}_n([R(X_0), \widehat{R}_c(X_0)], Y_0) + \lambda_C \mathbb{V}_n(R(X_0), \widehat{R}_c(X_0)) + \lambda_{E,0} \mathbb{D}_n(R(X_0) \| \gamma_{r_t})$.

We summarize the implementation of TESR in Algorithm 1. After obtaining the representation $[\widehat{R}_c, \widehat{R}_t]$, we can build predictive models based on the representation.

Algorithm 1 Transfer learning through Enhanced Sufficient Representation

Input: The source datasets $\mathcal{D}_s = \{Y_s, X_s\}$ for $s = 1, \dots, S$ and the target dataset $\mathcal{D}_0 = \{Y_0, X_0\}$, tuning parameter $\lambda_E, \lambda_Z, \lambda_C, \lambda_{E,0}$.

Step I: Estimating SIRep R_c with source datasets

1: With the source datasets \mathcal{D}_s with $s = 1, \dots, S$, we learn R_c with the following objectives,

$$\widehat{R}_c = \operatorname{argmin}_{R \in \mathcal{F}_{R_c}} \mathcal{L}_{S,n}(R), \quad (13)$$

where \mathcal{F}_{R_c} is the neural network class for learning R_c , $\mathcal{L}_{S,n}(R) = \sum_{s=1}^S \left\{ -\mathbb{V}_n(R(X_s), Y_s) + \lambda_E \mathbb{D}_n(R(X_s) \| \gamma_{r_c}) \right\} + \lambda_Z \mathbb{V}_n(R(X_{pool}), Z)$, Z is the one-hot domain indicator and X_{pool} is the pooled covariates for datasets with $s = 1, \dots, S$.

Step II: Estimating R_t with target dataset

1: For a given estimator \widehat{R}_c based on the source datasets, we learn R_t with the target dataset $\mathcal{D}_0 = \{Y_i, X_i\}$ to augment \widehat{R}_c . Specifically,

$$\widehat{R}_t = \operatorname{argmin}_{R \in \mathcal{F}_{R_t}} \mathcal{L}_{T,n}([R, \widehat{R}_c]),$$

where \mathcal{F}_{R_t} is the neural network class and $\mathcal{L}_{T,n}(R, \widehat{R}_c) = -\mathbb{V}_n([R(X_0), \widehat{R}_c(X_0)], Y_0) + \lambda_C \mathbb{V}_n(R(X_0), \widehat{R}_c(X_0)) + \lambda_{E,0} \mathbb{D}_n(R(X_0) \| \gamma_{r_t})$.

Output: The estimated representation $[\widehat{R}_c, \widehat{R}_t]$.

3.4 Linear representations

To better illustrate the concept of the proposed TESR framework, we consider the case where all the representation functions are linear in this section.

- A linear sufficient representation $R_s(X_s) = B_s^\top X_s$ for the s th source dataset satisfies $Y_s \perp\!\!\!\perp X_s \mid B_s^\top X_s$, where $B_s \in \mathbb{R}^{d \times r_s}$ and $B_s^\top B_s = I_{r_s}$.
- A linear sufficient and invariant representation $R_c(X) = B_c^\top X$ satisfies

$$Y_s \perp\!\!\!\perp X_s \mid B_c^\top X_s, \text{ for } s = 1, \dots, S, \text{ s.t. } B_c^\top X_{pool} \perp\!\!\!\perp Z, \quad (14)$$

where $B_c \in \mathbb{R}^{d \times r_c}$ and $B_c^\top B_c = I_{r_c}$, X_{pool} is the pooled covariates from different sources and Z is the source indicator.

The invariance constraint $B_c^\top X_{pool} \perp\!\!\!\perp Z$ ensures that B_c contains stable knowledge encoded in the predictors. The orthogonality condition $B_c^\top B_c = I_{r_c}$ is similar to the normality constraint (7) for nonlinear representation functions. These constraints help in achieving a stable and interpretable representation by ensuring that the learned features are orthogonal, which is crucial for maintaining the disentanglement and regularity properties.

Similar to (8), B_c can be defined as a solution of the optimization problem,

$$B_c^* \in \operatorname{argmin}_{B_c \in \mathbb{R}^{d \times r_c}} \sum_{s=1}^S \left\{ -\mathbb{V}(B_c^\top X_s, Y_s) + \lambda_E \|B_c^\top B_c - \mathbf{I}_{r_c}\|^2 \right\} + \lambda_Z \mathbb{V}(B_c^\top X_{pool}, Z),$$

where λ_E and λ_Z are regularization parameters. A trivial solution for summarizing the information from the sources is the stacked matrix $[B_1, \dots, B_S]$. However, the sources usually share some similarities, leading to the matrix $[B_1, \dots, B_S]$ not being of full rank. Therefore, it is preferred to seek a more concise representation that leverages these similarities among the sources efficiently. To this end, it is sufficient to learn the B_c which is the basis of the space spanned by $[B_1, \dots, B_S]$. This approach aligns with the findings presented in Xu et al. (2022) for the analysis of dimension reduction with heterogeneous sub-datasets.

With the B_c from the source domains that satisfies (14), our goal is to learn a $B_t \in \mathbb{R}^{d \times r_t}$ augmenting B_c such that $[B_c, B_t]$ is sufficient and $B_c \perp B_t$. This can be stated as

$$Y_0 \perp X_0 \mid [B_c^\top X_0, B_t^\top X_0] \text{ s.t. } B_c^\top B_t = \mathbf{0}.$$

The B_t can be characterized as a solution to the optimization problem

$$B_t^* \in \operatorname{argmin}_{B_t \in \mathbb{R}^{d \times r_t}} \left\{ -\mathbb{V}([B_c^\top X_0, B_t^\top X_0], Y_0) + \lambda_{E,0} \|B_t^\top B_t - \mathbf{I}_{r_t}\|^2 + \lambda_C \|B_c^\top B_t\|^2 \right\},$$

where $\lambda_{E,0}$ and λ_C are tuning parameters. The solutions B_c^* and B_t^* are typically non-unique, but all solutions lead to the same central subspace (Ma and Zhu, 2013; Xu et al., 2022). We refer to the Section A.2 of the Supplementary Materials for more details.

The method of linear sufficient dimension reduction using distance covariance has been discussed by Sheng and Yin (2016, 2013). The linear cases discussed above serve as an illustration of the concept of TESR. However, the intrinsic structures in real-world data are usually more complex and cannot be precisely represented by linear combinations of predictors. Nonlinear representations allow for a more flexible and comprehensive characterization of the underlying data structures.

4 Theoretical Guarantees

Under the framework of empirical risk minimization, the performance of the empirical risk minimizer $[\widehat{R}_c, \widehat{R}_t]$ can be evaluated by the excess risk. In this section, we establish the rate for the excess risk of the proposed TESR method.

Theoretical results are influenced by several factors, including the properties of R_c, R_t , the neural network classes $\mathcal{F}_{R_c}, \mathcal{F}_{R_t}$, the sample sizes of sources n_s and target datasets n_0 . We introduce some mild theoretical conditions on these factors, which are commonly considered in the deep learning literature. For further explanation and technical details regarding the function class and neural network classes, please refer to Section A of the Supplementary Materials.

We first have assumptions on the data distributions,

Assumption 1 *Let μ_X be the probability measure of the covariates. The $\operatorname{supp}(\mu_X)$ is contained in a compact set, say $[-B, B]^d$ with a finite B and denote its density function as $f_X(x)$. Y is bounded almost surely, say $\|Y\| \leq C$ a.s..*

Then we introduce the conditions on the representation functions. Recall that we are interested in $R_c = [R_{c,1}, \dots, R_{c,r_c}]$, $R_t = [R_{t,1}, \dots, R_{t,r_t}]$, and $R_0 = [R_{0,1}, \dots, R_{0,r_0}]$. In this paper, we assume that these functions belong to $B_{p,q,\tilde{\beta}}^\beta(\Omega)$, the anisotropic Besov (a-Besov) function class where $\beta = (\beta_1, \dots, \beta_d)^\top \in \mathbb{R}_+^d$ is the non-negative smoothness indices on the direction of d coordinates, $\tilde{\beta}$ is the average smoothness, $\tilde{\beta} = (\sum_{k=1}^d 1/\beta_k)^{-1}$, Ω is the domain and p, q are norm indices (Suzuki and Nitanda, 2021). The coordinate mixed smoothness provides insights for overcoming the curse of dimensionality (Suzuki and Nitanda, 2021). For simplicity, in the following analysis, we omit the β and denote the a-Besov space as $B_{p,q,\tilde{\beta}}$ as the $\tilde{\beta}$ directly impacts the final convergence analysis for the deep neural network estimator. We refer to the Section B.1 for more details of the a-Besov class.

We make the following assumptions on the structure of the functions.

Assumption 2 (Smoothness of representation functions) *All elements of representation functions $R_c : \mathbb{R}^d \rightarrow \mathbb{R}^{r_c}$, $R_t : \mathbb{R}^d \rightarrow \mathbb{R}^{r_t}$, $R_0 : \mathbb{R}^d \rightarrow \mathbb{R}^{r_0}$, belong to a-Besov spaces. Specifically,*

- (i) Write $R_c = [R_{c,1}, R_{c,2}, \dots, R_{c,r_c}]$. Assume that $R_{c,k} \in B_{p,q,\tilde{\beta}_{c,k}}$ where $\tilde{\beta}_{c,k}$ is the smoothness index, $k = 1, \dots, r_c$. Denote $\tilde{\beta}_c = \min\{\tilde{\beta}_{c,1}, \dots, \tilde{\beta}_{c,r_c}\}$.
- (ii) Write $R_t = [R_{t,1}, R_{t,2}, \dots, R_{t,r_t}]$. Assume that $R_{t,k} \in B_{p,q,\tilde{\beta}_{t,k}}$ where $\tilde{\beta}_{t,k}$ is the smoothness index, $k = 1, \dots, r_t$. Denote $\tilde{\beta}_t = \min\{\tilde{\beta}_{t,1}, \dots, \tilde{\beta}_{t,r_t}\}$.
- (iii) Write $R_0 = [R_{0,1}, R_{0,2}, \dots, R_{0,r_0}]$. Assume $R_{0,k} \in B_{p,q,\tilde{\beta}_{0,k}}$, $k = 1, \dots, r_0$. Denote $\tilde{\beta}_0 = \min\{\tilde{\beta}_{0,1}, \dots, \tilde{\beta}_{0,r_0}\}$.

Assumption 2 requires that all these representations belong to the a-Besov classes with different smoothness parameters. The a-Besov function space includes many popular classes, such as Hölder class and Besov class. Thus, the theoretical studies in our work are general and applicable to various problems. As we mentioned before, the function R_t usually has a much simpler structure than R_0 , which means $\tilde{\beta}_t > \tilde{\beta}_0$.

Since the a-Besov function classes are considered, Suzuki and Nitanda (2021) proves that the deep neural network from the ReLU neural network function class \mathcal{F} can effectively learn functions from the a-Besov class where \mathcal{F} is the function class of the feed-forward neural network with the Rectified Linear Unit (ReLU) activation function (Schmidhuber, 2015). Let $\mathcal{F} \equiv \mathcal{F}(\theta, \mathcal{H}, \mathcal{W}, \mathcal{S})$ be the set of such ReLU neural networks $R : \mathbb{R}^d \rightarrow \mathbb{R}^r$ with weights θ , depth \mathcal{H} , width \mathcal{W} and size \mathcal{S} . Here the depth \mathcal{H} refers to the number of hidden layers. A $(\mathcal{H} + 1)$ -vector $(w_0, w_1, \dots, w_{\mathcal{H}})$ denotes the width of each layer. The width $\mathcal{W} = \max\{w_1, \dots, w_{\mathcal{H}}\}$ is the maximum width of the hidden layers. The size $\mathcal{S} = \sum_{i=0}^{\mathcal{H}} [w_i \times w_{i+1}]$ is the total number of parameters in the network. In this paper, we denote \mathcal{F}_{R_c} , \mathcal{F}_{R_t} as the network classes for learning R_c and R_t , respectively. Then we give the specification as follows.

Assumption 3 (Neural network classes for learning R_c and R_t) *Recall that N denotes total sample size on the source datasets. The neural network classes \mathcal{F}_{R_c} , \mathcal{F}_{R_t} for learning R_c and R_t is defined as follows,*

- (i) We denote \mathcal{F}_{R_c} as the deep neural network class for learning the R_c . We set the depth $\mathcal{H}_{R_c} = \mathcal{O}(\log(d) \log(N))$, width $\mathcal{W}_{R_c} = \mathcal{O}(r_c d N^{1/(2\tilde{\beta}_c+1)})$, model size $\mathcal{S}_{R_c} = \mathcal{O}(r_c d^2 N^{1/(2\tilde{\beta}_c+1)} \log(N) \log(d))$.

(ii) We denote \mathcal{F}_{R_t} as the deep neural network class for learning the R_t . We set the depth $\mathcal{H}_{R_t} = \mathcal{O}(\log(d) \log(n_0))$, width $\mathcal{W}_{R_t} = \mathcal{O}(r_t d n_0^{1/(2\tilde{\beta}_t+1)})$, model size $\mathcal{S}_{R_t} = \mathcal{O}(r_t d^2 n_0^{1/(2\tilde{\beta}_t+1)} \log(n_0) \log(d))$.

We note that the possible network structures are not unique, and these network structures are not designed to be optimal due to the possible heterogeneity in smoothness among the components of the representation functions.

In the following Lemma 4.1, we give the convergence result for \widehat{R}_c with the source datasets.

Lemma 4.1 (Convergence result of learning representation on sources) Denote R_c^* as a solution of (7). Set the tuning parameter $\lambda_E, \lambda_Z = \mathcal{O}(1)$, with Assumption 1-3, we have the excess risk bound for the \widehat{R}_c ,

$$\mathcal{L}_S(\widehat{R}_c) - \mathcal{L}_S(R_c^*) = \widetilde{\mathcal{O}}(r_c^{1/2} N^{-\frac{\tilde{\beta}_c}{2\tilde{\beta}_c+1}}).$$

Remark 1 The α -Besov space includes the Hölder class as a special case (Suzuki and Nitanda, 2021). If the components of R_c are from the Hölder class with smoothness index β , then we have $\tilde{\beta}_{c,k} = \beta/d$ for $k = 1, \dots, r_c$. Under this condition, the convergence rate derived in Lemma 4.1 is $\widetilde{\mathcal{O}}(r_c^{1/2} N^{-\frac{\beta}{2\beta+d}})$. The convergence rate deteriorates with increasing dimension d , which is caused by the curse of dimensionality.

Finally, we provide the bound for the excess risk of $[\widehat{R}_c, \widehat{R}_t]$ on the target domain \mathcal{D}_0 .

Theorem 1 (Convergence result of TESR on the target domain) Denote $[R_c^*, R_t^*]$ as a solution of expression (10). Set the tuning parameter $\lambda_E, \lambda_Z = \mathcal{O}(1)$, with Assumption 1-3 and the conditions in Lemma 4.1, we have the excess risk bound for the $[\widehat{R}_c, \widehat{R}_t]$ on the \mathcal{D}_0 ,

$$\mathcal{L}_T([\widehat{R}_c, \widehat{R}_t]) - \mathcal{L}_T([R_c^*, R_t^*]) = \widetilde{\mathcal{O}}(r_t^{1/2} n_0^{\frac{-\tilde{\beta}_t}{2\tilde{\beta}_t+1}}) + \widetilde{\mathcal{O}}(r_c^{1/4} N^{-\frac{\tilde{\beta}_c/2}{2\tilde{\beta}_c+1}}).$$

Under the same conditions, it can be shown that estimating R_0 using only the target dataset \mathcal{D}_0 leads to the excess risk with order $\widetilde{\mathcal{O}}(r_0^{1/2} n_0^{\frac{-\tilde{\beta}_0}{2\tilde{\beta}_0+1}})$, which can be derived using a similar approach as outlined in Lemma 4.1. We compare the excess risk of the TESR and the excess risk of the estimated representation that only uses the target dataset. The ratio of these two excess risks is

$$\frac{\text{excess risk of TESR}}{\text{excess risk of only using target data}} = \widetilde{\mathcal{O}}\left(\frac{r_t^{1/2}}{r_0^{1/2}} n_0^{\frac{\tilde{\beta}_0 - \tilde{\beta}_t}{(2\tilde{\beta}_0+1)(2\tilde{\beta}_t+1)}}\right) + \widetilde{\mathcal{O}}\left(\frac{r_c^{1/4}}{r_0^{1/2}} N^{-\frac{\tilde{\beta}_c/2}{2\tilde{\beta}_c+1}} n_0^{\frac{\tilde{\beta}_0}{2\tilde{\beta}_0+1}}\right). \quad (15)$$

The second term in expression (15) is $o(1)$ with $N \gg n_0$ in the context of transfer learning. So we can focus on the the first term.

The proposed transfer learning method outperforms the method without using the source datasets if $r_t^{1/2} r_0^{-1/2} n_0^{\frac{\tilde{\beta}_0 - \tilde{\beta}_t}{(2\tilde{\beta}_0+1)(2\tilde{\beta}_t+1)}} = o(1)$. This holds if $\tilde{\beta}_t > \tilde{\beta}_0$. This is true if the additional component R_t is smoother than R_0 , the sufficient representation on the target domain. We also note that the rate of the first term in (15) can be improved if $r_t/r_0 = o(1)$, which signifies that the majority of the useful information is already included in R_c . Therefore, the intrinsic dimension of R_t is smaller than that of R_0 . Existing transfer learning methods mainly focus on reducing complexity, often defined in terms of smoothness or sparsity (Cai and Pu, 2022; Tian and Feng, 2023). However, these approaches often overlook the role of knowledge volume, which is typically represented by model size and the number of latent representations.

5 Simulation Studies

In this section, we evaluate the performance of TESR. As TESR focuses on constructing data representations rather than making direct predictions, we assess its effectiveness using the results from a predictive model that takes inputs $[\widehat{R}_c, \widehat{R}_t]$ generated by TESR. We compare its performance against the following existing methods.

- **Deep Neural Network-based Classifier (DNN)** (Schmidhuber, 2015): the classical end-to-end deep neural network based classifier with logistic loss, relying only on the target dataset.
- **Deep Dimension Reduction (DDR)** (Huang et al., 2024): a supervised learning representation method that learns representations based on deep neural networks and distance covariance, relying solely on the target dataset. Similar to other methods, its performance is assessed using numerical results from a predictive model that takes the learned representation as input.
- **TransIRM**: a **T**ransfer learning method based on **I**nvariant **R**isk **M**inimization (Arjovsky et al., 2019). Specifically, we learn the invariant representation from the source datasets using the invariant regularization proposed by Arjovsky et al. (2019). The invariant representation is fixed and taken as input for an deep neural network classifier which are trained using the logistic loss on the target dataset. A key difference between TESR and the TransIRM is that TESR takes into account the specific information in the target domains while the TransIRM does not.

All the experiments in this section were replicated 100 times. These methods mentioned above were implemented using the same network architecture and model size to ensure fair comparisons. The dimension of the representation estimator $\widehat{R}_c, \widehat{R}_T$ are set to 32 in all the simulations. Implementation details of these methods are given in Section C of the Supplementary Materials.

5.1 Example 1: Models with various (n_s, n_0, d)

We evaluate the performance of TESR and compare it with existing methods by considering various combinations of (n_s, n_0, d) .

- **Target domain**: the target domain model is a binary classification model with $Y_0 \in \{0, 1\}$ and $X_0 \in \mathbb{R}^d$. The model is

$$P(Y_0 = 1 | X_0 = x) = \frac{\exp[g(x)]}{1 + \exp[g(x)]},$$

where $g(x) = g_0(x) - \mathbb{E}(g_0(X_0))$ with $g_0(x) = 2f_1(x_1) + f_2(x_2, x_3) + f_3(x_3, x_4) + f_4(x_4, x_5)$. Here the component functions are $f_1(u) = (u-0.9)^2$, $f_2(u, v) = -uv(u-0.5)^2$, $f_3(u, v) = \sin(-0.2\pi uv) + 1$, $f_4(u, v) = u(|v| + 1)^2$, $f_5(u) = \sin(0.5\pi u) + 1$, $f_6(u) = 2 \sin(\pi u)/(2 - \sin(\pi u))$.

- **Source domains**: source domain models are regression models with $Y_s \in \mathbb{R}$ and $X_s \in \mathbb{R}^d$, $s = 1, \dots, 4$. The regression functions in the source domains are given below,

- $\mathcal{D}_1 : y = 3f_1(x_1) + f_2(x_2, x_3) + f_3(x_3, x_4) + f_5(x_6) + \epsilon_1;$
- $\mathcal{D}_2 : y = 3f_1(x_1) + f_2(x_2, x_3) + f_3(x_3, x_4) + 2f_5(x_6) + \epsilon_2;$
- $\mathcal{D}_3 : y = 2f_1(x_1) + 1.5f_2(x_2, x_3) + f_3(x_3, x_4) + f_6(x_7) + \epsilon_3;$
- $\mathcal{D}_4 : y = 2f_1(x_1) + 1.5f_2(x_2, x_3) + f_3(x_3, x_4) + 2f_6(x_7) + \epsilon_4.$

Across all the five domains, the covariates $x \sim N(\mathbf{0}, \Sigma)$ where $\Sigma_{i,j} = 0.2^{|i-j|}$ for $i, j = 1, \dots, d$. For $s = 1, 2, 3, 4$, ϵ_s are independently drawn from $N(0, 0.5^2)$. In Example 1, f_1, f_2, f_3 are the shared components but their coefficients vary across the five domains. We note that x_5 is the unique information for the target domain \mathcal{D}_0 and x_6, x_7 is only active in the source domains $\mathcal{D}_S, s = 1, 2, 3, 4$.

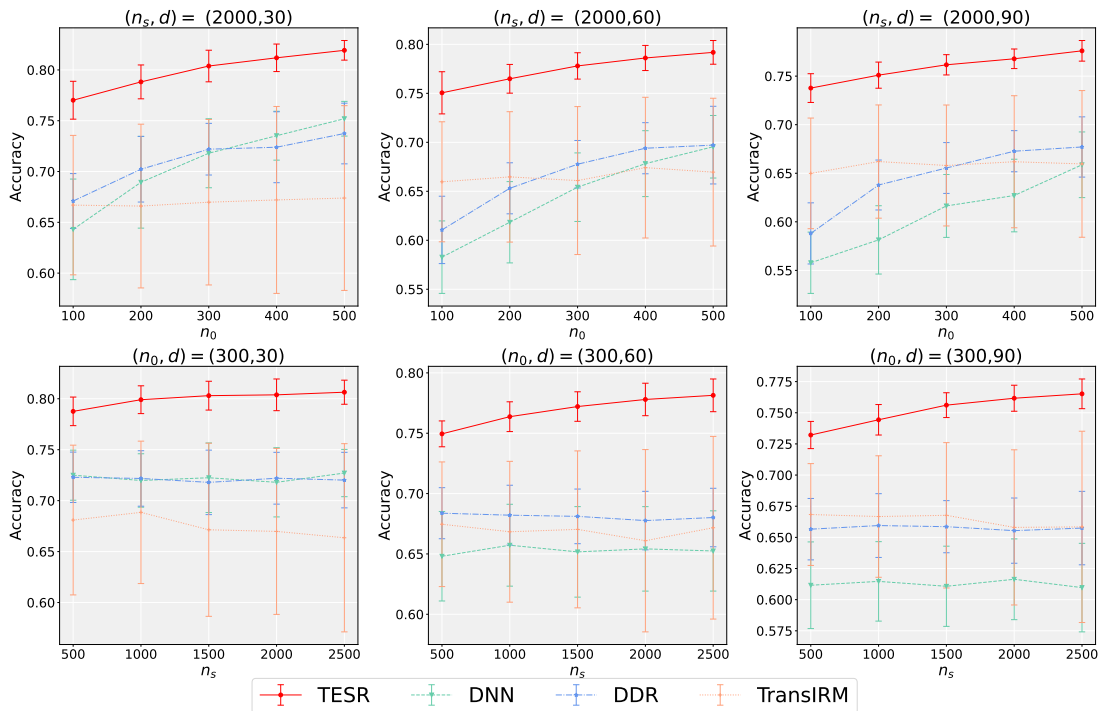


Figure 3: Classification accuracy and its standard deviation (represented by the width of the error bar) for the four methods, TESR, DNN, DDR, and TransIRM, are evaluated with various values of (n_s, n_0, d) over 100 replications in Example 1.

Figure 3 shows the classification accuracy and its standard deviation across 100 replications. Notably, TESR consistently outperforms all its competitors. As the source sample size increases, TESR’s performance improves significantly, while TransIRM’s performance fluctuates. Furthermore, by effectively capturing specific information from the target, TESR becomes significantly more efficient than TransIRM as the target sample size increases. TransIRM surpasses DDR and DNN when the dimensionality d is large and the target data size n_0 is relatively small. However, it remains significantly less effective compared to TESR.

To further demonstrate the efficiency of TESR, we examine its performance across different designs of dimensions for the representation functions $[\widehat{R}_c, \widehat{R}_t]$ in Table 1. TESR maintains stable performance with varying r^* where $r^* = \dim(\widehat{R}_c) = \dim(\widehat{R}_t)$. TESR consistently outperforms all competitors with higher accuracy and smaller standard deviation.

Table 1: The classification accuracy and its standard deviation with $(n_s, n_0, d) = (2000, 300, 60)$ and different r^* , dimensions of the representation estimator modules in Example 1.

r^*	TESR	DNN	DDR	TransIRM
8	0.782 (0.015)	0.661 (0.036)	0.676 (0.021)	0.602(0.092)
16	0.783 (0.015)	0.664 (0.032)	0.673 (0.023)	0.639(0.086)
32	0.784 (0.014)	0.652 (0.036)	0.677 (0.019)	0.653(0.075)
64	0.783 (0.013)	0.657 (0.033)	0.673 (0.027)	0.652(0.072)

Additionally, we also consider a case where the sources and target are all regression problems in Example S.1 of the Supplementary Materials.

5.2 Example 2: Models with two target tasks

In this section, we examine the performance of the proposed method on two independent target tasks, showing that its effectiveness is independent of regression function similarity. Specifically, we generate 4 sources and 2 target datasets.

- Target domains: there are two target domains, both have a binary response variable. The first target domain model is,

$$P(Y_{01} = 1|X_{01} = x) = \frac{\exp[g_1(x)]}{1 + \exp[g_1(x)]},$$

where $g_1(x) = g_{01}(x) - \mathbb{E}(g_{01}(X_{01}))$, with $g_{01}(x) = 2f_1(x_1) + f_2(x_2, x_3) + f_3(x_3, x_4) + f_4(x_4, x_5)$. The second target domain model is generated from

$$P(Y_{02} = 1|X_{02} = x) = \frac{\exp[g_2(x)]}{1 + \exp[g_2(x)]},$$

where $g_2(x) = g_{02}(x) - \mathbb{E}(g_{02}(X_{02}))$ with $g_{02}(x) = 2f_1(x_8) + f_2(x_9, x_{10}) + f_3(x_{10}, x_{11}) + f_4(x_{11}, x_{12})$. The two target tasks are independent and depend on entirely different covariates.

- Source domains: regression models with $Y_s \in \mathbb{R}$ and $X_s \in \mathbb{R}^d$, $s = 1, \dots, 4$. The regression functions are given below,

- $\mathcal{D}_1 : y = f_1(x_1) + 2f_2(x_9, x_{10}) + 2f_3(x_{10}, x_{11}) + f_5(x_6) + \epsilon_1$;
- $\mathcal{D}_2 : y = f_1(x_1) + 2f_2(x_9, x_{10}) + 2f_3(x_{10}, x_{11}) + 2f_5(x_6) + \epsilon_2$;
- $\mathcal{D}_3 : y = f_1(x_8) + 2f_2(x_2, x_3) + 2f_3(x_3, x_4) + 2f_5(x_{13}) + \epsilon_3$;
- $\mathcal{D}_4 : y = f_1(x_8) + 2f_2(x_2, x_3) + 2f_3(x_3, x_4) + 2f_5(x_{13}) + \epsilon_4$,

where covariates and the error terms are generated from standard Gaussian distribution and the component functions the same as that in Example 1.

Figure 4 reports the classification accuracy on tasks T_1, T_2 of the 4 methods. TESR achieves the best accuracy on both target tasks. TESR learns the sufficient and invariant representation R_c from the sources, which effectively captures generalizable features despite the high heterogeneity among the sources. However, in contrast to Example 1, TransIRM performs consistently worse

than the other methods in Example 2. One possible explanation is that the invariant loss proposed by Arjovsky et al. (2019) is unable to capture robust information from these highly heterogeneous sources effectively. In conclusion, TESR, which incorporates representations with theoretical guarantees, can draw information from the heterogeneous sources and enhance the performance on different down-streaming tasks.

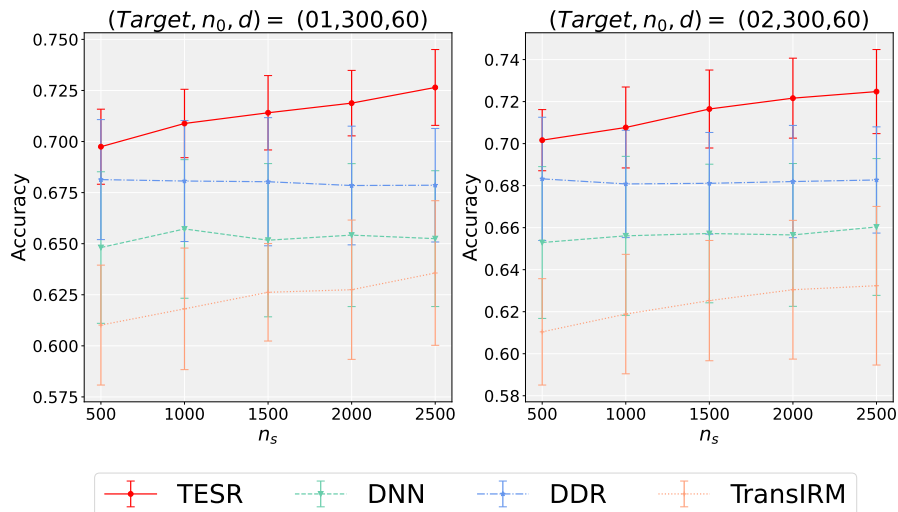


Figure 4: Classification accuracy and its standard deviation (width of error bar) on the two independent target tasks in Example 2.

The proposed method can capture the heterogeneous information from sources and enhance the performance of independent target tasks, unlike the conventional transfer learning methods which depend on high degree of similarity on regression function. Different downstream tasks benefit from the specific components of the multi-dimensional sufficient representation. Furthermore, the highly structured features preserved in these representation functions provide valuable insights into the success of pre-trained models across diverse downstream tasks.

5.3 Example 3: Models with heterogeneity between source and target domains

In Example 3, we examine how the performance of TESR is affected by increasing heterogeneity between the source domains and the target domain.

- Target domain: the target domain model is a binary classification model, which takes the form:

$$P(Y_0 = 1|X_0 = x) = \frac{\exp[g(x)]}{1 + \exp[g(x)]},$$

where $g(x) = g_0(x) - \mathbb{E}(g_0(X_0))$ with $g_0(x) = 2f_1(x_1) + f_2(x_2, x_3) + f_3(x_3, x_4) + f_4(x_4, x_5)$.

- Source domains: source domains models are regression models:

$$\mathcal{D}_s : y = 2\gamma_{s,1}f_1(x_1) + \gamma_{s,2}\left[f_2(x_2, x_3) + f_3(x_3, x_4)\right] + 2f_5(x_6) + \epsilon_s, \quad s = 1, \dots, 8,$$

where x is drawn from a standard Gaussian distribution, and the component functions f_1, \dots, f_5 and error terms are the same as those in Example 1. The coefficients $(\gamma_{s,1}, \gamma_{s,2})$ control the differences between the functions in \mathcal{D}_s and \mathcal{D}_0 . When $\gamma_{s,1} = \gamma_{s,2} = 1$, the shared components of target model and source model functions are identical. Any deviation from these values introduces heterogeneity between target and source models.

We consider two types of departures with coefficients $(\gamma_{s,1}, \gamma_{s,2})$.

- For the source index $s = 1, \dots, 6$,
 - Type I (**L_1 distance**): $(\gamma_{s,1}, \gamma_{s,2}) = (1 + 0.5s, 1 + 0.5s)$;
 - Type II (**cosine distance**): $(\gamma_{s,1}, \gamma_{s,2}) = (\cos(s\pi/3) - \sin(s\pi/3), \cos(s\pi/3) + \sin(s\pi/3))$;
- For the source index $s = 7, 8$, in both Type I and II: $(\gamma_{s,1}, \gamma_{s,2}) = (0, 0)$.

Under the Type I departure, the L_1 distance among the regression functions from \mathcal{D}_s and \mathcal{D}_0 increases with s (Cai and Pu, 2022). Meanwhile, under the Type II departure, the cosine distance changes with s (Gu et al., 2024). Details of the L_1 and cosine distances between the regression functions from \mathcal{D}_s and \mathcal{D}_0 are reported in Section C of Supplementary Materials. In short, the departure on regression functions of \mathcal{D}_s from \mathcal{D}_0 increases with s . Notably, the datasets \mathcal{D}_7 and \mathcal{D}_8 are entirely redundant and offer no benefit for the target.

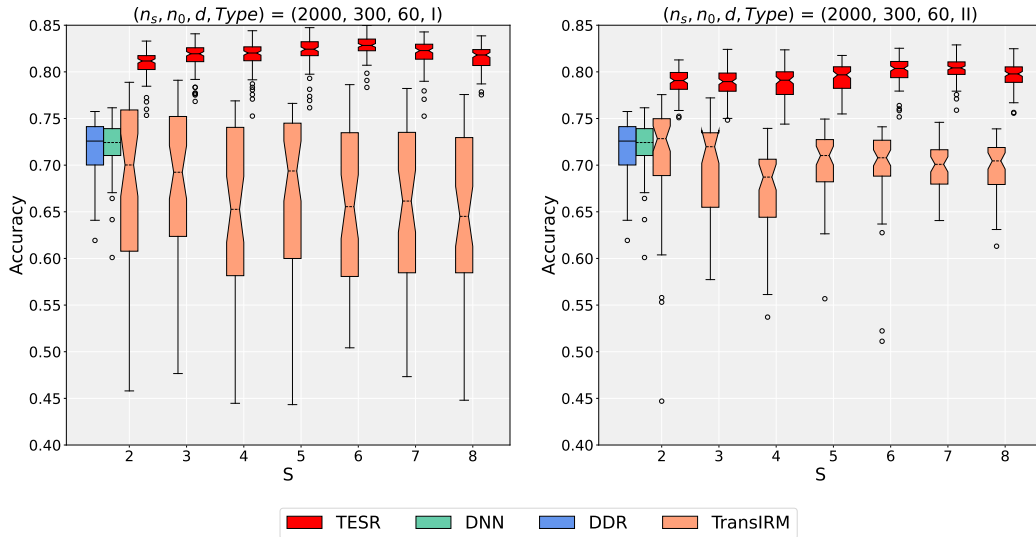


Figure 5: The box plot illustrates classification accuracy over 100 replications on the target dataset in Example 3, under L_1 (left panel) and cosine distance departure (right panel) conditions, where source datasets are sequentially added into the modeling process. TESR (notched box with solid line) outperforms TransIRM (notched box with solid line), DDR (rectangular box with solid line), and DNN (rectangular box with dashed line). DDR and DNN are only presented once, as they do not utilize the source information.

In Example 3, we sequentially incorporate source datasets into the model and evaluate the performance of four methods. Figure 5 displays the classification accuracy over 100 replications. TESR consistently outperforms the other methods in both scenarios, with its performance improving as additional sources ($s = 2, \dots, 6$) are included. However, as more sources are added, the heterogeneity among them increases, making it more challenging for TransIRM to capture invariant features. Despite this, TESR maintains satisfactory performance and proves particularly advantageous for analyzing large-scale datasets, where eliminating redundant sources using complex source selection algorithms can be computationally intensive (Cai and Pu, 2022; Li et al., 2022).

We take a closer look at the Type I departure case. For $s = 1, \dots, 6$, the coefficients $(\gamma_{s,1}, \gamma_{s,2})$ of the components $f_1(x_1)$ and $(f_2(x_2, x_3) + f_3(x_3, x_4))$ increase with s . As s increases, the L_1 distance between the regression functions from \mathcal{D}_s and \mathcal{D}_0 increases, leading to larger discrepancy between their regression functions (Li et al., 2022; Tian and Feng, 2023). Conventional transfer learning methods regard these sources with large distance from the target task \mathcal{D}_0 as redundant and introduce sophisticated source selection algorithms to remove them. However, large coefficients $(\gamma_{s,1}, \gamma_{s,2})$ lead to a higher signal-to-noise ratio on sources which is expected to facilitate the learning of representations. As shown in the left panel of Figure 5, the classification accuracy of TESR improves as additional sources are included. A similar conclusion can also be drawn from the cases under Type II departures as shown in the right panel of Figure 5, although $(\gamma_{s,1}, \gamma_{s,2})$ may vary between positive and negative under Type II departures (Gu et al., 2024).

In conclusion, even though the source domain regression functions with diverse coefficients $(\gamma_{s,1}, \gamma_{s,2})$ differ significantly from the target domain function for classification, they still offer valuable knowledge for the target task. TESR, by achieving knowledge transfer through representation functions, is capable of capturing valuable information from these heterogeneous sources.

6 Real data examples

In this section, we evaluate TESR in terms of prediction and classification performance on two datasets, comparing it with existing methods: DDN, DDR, and TransIRM. The datasets used for this evaluation include a gene expression dataset and an image dataset.

6.1 Prediction of JAM2 gene expression

Primary familial brain calcification (PFBC) is an infrequent, autosomal dominant neurological disorder, distinguished by the presence of bilateral calcifications within the basal ganglia and additional cerebral areas. Recent studies have identified the gene JAM2 as a novel causative gene of autosomal recessive PFBC (Cen et al., 2020; Schottlaender et al., 2020). JAM2 encodes junctional adhesion molecule 2, which is highly expressed in neurovascular unit-related cell types, such as endothelial cells and astrocytes, and is predominantly localized on the plasma membrane. Schottlaender et al. (2020) have illustrated that specific genetic variants result in diminished levels of JAM2 mRNA expression and an absence of the JAM2 protein in fibroblasts derived from patients, aligning with a loss-of-function mechanism. Consequently, predicting the expression level of JAM2 in target brain tissues is of significant interest.

We utilize TESR to construct models for each tissue to predict the expression level of JAM2, using data from the Genotype-Tissue Expression (GTEx) project (Consortium et al., 2015). In

the GTEx project, genes related to the central nervous system are organized into MODULE 137, which includes 13 tissues and a total of 545 genes, along with an additional 1,632 genes that are significantly enriched in the same experiments as the module’s genes. Table 2 provides the sample sizes of the datasets across the various tissues. These datasets are available at <https://gtexportal.org/home/>.

Table 2: The sample size of the datasets across the tissues

Target task	Full name	Sample size
Amygdala	Brain_Amygdala	152
Anterior	Brain_Anterior_cingulate_cortex_BA24	176
Caudate	Brain_Caudate_basal_ganglia	246
Cerebellar	Brain_Cerebellar_Hemisphere	215
Cerebellum	Brain_Cerebellum	241
Cortex	Brain_Cortex	255
Frontal	Brain_Frontal_Cortex_BA9	209
Hippocampus	Brain_Hippocampus	197
Hypothalamus	Brain_Hypothalamus	202
Nucleus	Brain_Nucleus_accumbens_basal_ganglia	246
Putamen	Brain_Putamen_basal_ganglia	205
Spinal	Brain_Spinal_cord_cervical_c-1	159
Substantia	Brain_Substantia_nigra	139
Average		203

To predict the expression level of JAM2 in a specific tissue, we utilize data from other tissues as source datasets. For each target tissue dataset, we employ 5-fold cross-validation, allocating 60% of the data for training, 20% for evaluation, and 20% for testing. The source datasets are divided into training and evaluation sets in a 4:1 ratio. We compare the results with existing methods through cross-validation.

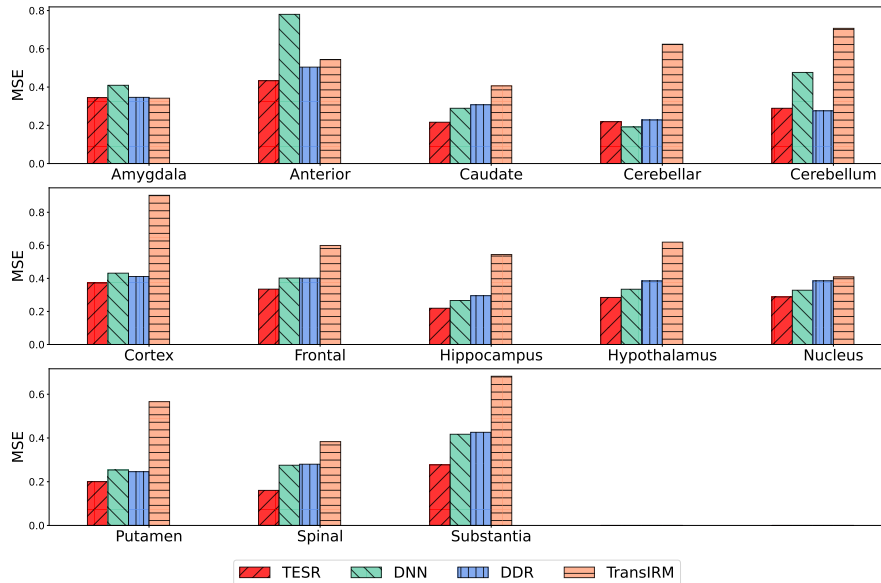


Figure 6: The Mean Square Error (MSE) averaged from 5-fold cross-validation on 13 different tissue groups. Each groups are denoted with their abbreviations.

The average MSE from 5-fold cross-validation is presented in Figure 6. TESR achieves the best performance in 10 out of the 13 tissues when compared to all other methods. In the *Amygdala*, *Cerebellar* and *Cerebellum* tissues, where TESR does not outperform the others, its performance remains competitive. The variations in performance across tissues may be attributed to the heterogeneity of information in the distributions of different tissues. Based on this experiment, we conclude that TESR effectively learns knowledge from relevant tasks, demonstrating its potential for broad applicability. The superiority of TESR over TransIRM also highlights the importance of adapting specific information from the target domain in transfer learning.

6.2 Image classification using PACS dataset

We use TESR to construct image classification models for each style within the PACS dataset, which includes images in four distinct styles: Photo (P), Art painting (A), Cartoon (C), and Sketch (S) (Li et al., 2017). Each style contains images across seven categories, as shown in the right panel of Figure 7. For this purpose, we utilize the CIFAR-10 dataset (Krizhevsky, 2009) as the source and each of the four styles of the PACS dataset as the target task. The source dataset comprises 10 classes, while the target datasets consist of 7 classes. As a result, conventional transfer learning methods that require the same data structure for source and target datasets are not well-suited to this scenario.

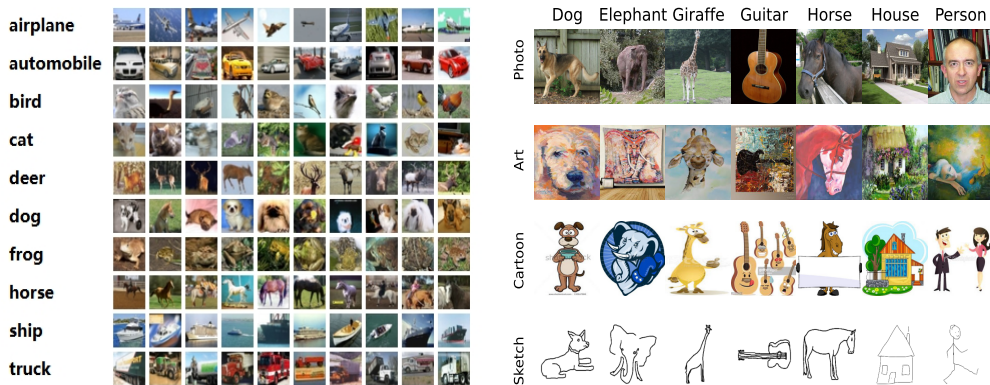


Figure 7: Examples from the CIFAR-10 (Left) and PACS (Right) datasets. We consider transferring the knowledge in CIFAR-10 to 4 domains of the PACS dataset.

Table 3: The accuracy of classification and its standard deviation (in brackets) on different targets.

	TESR	TransIRM	DDR	DNN
Photo	0.700 (0.038)	0.533 (0.062)	0.634 (0.035)	0.617 (0.030)
Art	0.488 (0.063)	0.401 (0.043)	0.336 (0.024)	0.411 (0.031)
Cartoon	0.720 (0.012)	0.430 (0.089)	0.672 (0.040)	0.669 (0.029)
Sketch	0.620 (0.047)	0.414 (0.101)	0.594 (0.037)	0.742 (0.024)

We use 5-fold cross-validation, allocating 60% of the target datasets for training, 20% for evaluation, and 20% for testing. For the source datasets, we use 80% for training and 20% for evaluation. The results are presented in Table 3. TESR outperforms TransIRM and DDR across the four different target domains and achieves superior performance compared to DNN, except for the Sketch data. One possible explanation is that the Sketch data contains fewer details and has a simpler structure, which can be effectively captured by simpler models, rendering the texture information from other domains less useful.

7 Conclusion and Discussion

In this paper, we introduce TESR, a transfer learning framework that leverages sufficient and invariant data representations to enhance learning across different domains. The core of our approach involves learning data representations from source tasks and enhancing them with an additional component designed to extract specific information for the target task. Unlike traditional transfer learning methods that rely heavily on critical source selection algorithms to ensure close alignment between source and target datasets, TESR allows the sufficient and invariant representations from the sources to be only partially relevant to, or even independent of, the target task. The augmenting component is capable of extracting relevant knowledge for the target domain. This flexibility enhances the generality and robustness of transfer learning, making it particularly effective for complex datasets where validating task similarities is infeasible or costly.

Several questions warrant further investigation. First, developing a data-driven approach based on cross-validation for selecting the dimensions of Sufficient and Invariant Representations (SIRep) for the source domains, as well as the augmenting representations from the target

domain, would be beneficial. Second, exploring alternative measures for conditional independence, such as mutual information, could provide deeper insights and enhance the framework's effectiveness. Third, it would be valuable to develop alternative methods for adapting the SIRep from the source domains to the target domain. For instance, while the proposed method involves enhancing SIRep with an independent component estimated from the target data, exploring other strategies could be fruitful. We leave these questions for future work.

References

- Anthony, M. and P. L. Bartlett (2009). *Neural Network Learning: Theoretical Foundations*. cambridge University Press.
- Arjovsky, M., L. Bottou, I. Gulrajani, and D. Lopez-Paz (2019). Invariant risk minimization. *arXiv preprint arXiv:1907.02893*.
- Bartlett, P. L., N. Harvey, C. Liaw, and A. Mehrabian (2019). Nearly-tight vc-dimension and pseudodimension bounds for piecewise linear neural networks. *Journal of Machine Learning Research* 20, 1–17.
- Bastani, H. (2021). Predicting with proxies: Transfer learning in high dimension. *Management Science* 67(5), 2964–2984.
- Bengio, Y., A. Courville, and P. Vincent (2013). Representation learning: A review and new perspectives. *IEEE Transactions on Pattern Analysis and Machine Intelligence* 35(8), 1798–1828.
- Cai, T. T. and H. Pu (2022). Transfer learning for nonparametric regression: Non-asymptotic minimax analysis and adaptive procedure. *arXiv preprint arXiv:2401.12272*.
- Cai, T. T. and H. Wei (2021). Transfer learning for nonparametric classification: minimax rate and adaptive classifier. *Annals of Statistics* 49(1), 100–128.
- Cen, Z., Y. Chen, S. Chen, H. Wang, D. Yang, H. Zhang, H. Wu, L. Wang, S. Tang, J. Ye, et al. (2020). Biallelic loss-of-function mutations in jam2 cause primary familial brain calcification. *Brain* 143(2), 491–502.
- Chen, Y., Y. Jiao, R. Qiu, and Z. Yu (2024). Deep nonlinear sufficient dimension reduction. *Annals of Statistics* 52(3), 1201 – 1226.
- Consortium, G., K. G. Ardlie, D. S. Deluca, A. V. Segrè, T. J. Sullivan, T. R. Young, E. T. Gelfand, C. A. Trowbridge, J. B. Maller, T. Tukiainen, et al. (2015). The genotype-tissue expression (gtex) pilot analysis: multitissue gene regulation in humans. *Science* 348(6235), 648–660.
- Cook, R. D. and L. Ni (2005). Sufficient dimension reduction via inverse regression: A minimum discrepancy approach. *Journal of the American Statistical Association* 100(470), 410–428.
- De la Pena, V. and E. Giné (2012). *Decoupling: from dependence to independence*. Springer Science & Business Media.

- Gretton, A., K. M. Borgwardt, M. J. Rasch, B. Schölkopf, and A. Smola (2012). A kernel two-sample test. *Journal of Machine Learning Research* 13(1), 723–773.
- Gu, T., Y. Han, and R. Duan (2024). Robust angle-based transfer learning in high dimensions. *Journal of the Royal Statistical Society Series B: Statistical Methodology*, qkae111.
- Hu, Z., Z. Zhao, X. Yi, T. Yao, L. Hong, Y. Sun, and E. Chi (2022). Improving multi-task generalization via regularizing spurious correlation. *Advances in Neural Information Processing Systems* 35, 11450–11466.
- Huang, J., Y. Jiao, X. Liao, J. Liu, and Z. Yu (2024). Deep dimension reduction for supervised representation learning. *IEEE Transactions on Information Theory* 70(5), 3583–3598.
- Huo, X. and G. J. Székely (2016). Fast computing for distance covariance. *Technometrics* 58(4), 435–447.
- Jiao, Y., H. Lin, Y. Luo, and J. Z. Yang (2024). Deep transfer learning: Model framework and error analysis. *arXiv preprint arXiv:2410.09383*.
- Krizhevsky, A. (2009). Learning multiple layers of features from tiny images. *Master’s thesis, University of Toronto*.
- Lee, K.-Y., B. Li, and F. Chiaromonte (2013). A general theory for nonlinear sufficient dimension reduction: Formulation and estimation. *Annals of Statistics* 41(1), 221 – 249.
- Li, D., Y. Yang, Y.-Z. Song, and T. M. Hospedales (2017). Deeper, broader and artier domain generalization. In *Proceedings of the IEEE international conference on computer vision*, pp. 5542–5550.
- Li, K.-C. (1991). Sliced inverse regression for dimension reduction. *Journal of the American Statistical Association* 86(414), 316–327.
- Li, S., T. T. Cai, and H. Li (2022). Transfer learning for high-dimensional linear regression: Prediction, estimation and minimax optimality. *Journal of the Royal Statistical Society Series B: Statistical Methodology* 84(1), 149–173.
- Ma, Y. and L. Zhu (2013). Efficient estimation in sufficient dimension reduction. *Annals of Statistics* 41(1), 250.
- Maurer, A., M. Pontil, and B. Romera-Paredes (2016). The benefit of multitask representation learning. *Journal of Machine Learning Research* 17(81), 1–32.
- Neyshabur, B., H. Sedghi, and C. Zhang (2020). What is being transferred in transfer learning? *Advances in Neural Information Processing Systems* 33, 512–523.
- Pan, S. J. and Q. Yang (2009). A survey on transfer learning. *IEEE Transactions on Knowledge and Data Engineering* 22(10), 1345–1359.
- Rizzo, M. L. and G. J. Székely (2016). Energy distance. *Wiley Interdisciplinary Reviews: Computational Statistics* 8, 27–38.

- Schmidhuber, J. (2015). Deep learning in neural networks: An overview. *Neural Networks* 61, 85–117.
- Schmidt-hieber, J. (2020). Nonparametric regression using deep neural networks with relu activation function. *Annals of Statistics* 48(4), 1875–1897.
- Schottlaender, L. V., R. Abeti, Z. Jaunmuktane, C. Macmillan, V. Chelban, B. O’callaghan, J. McKinley, R. Maroofian, S. Efthymiou, A. Athanasiou-Fragkouli, et al. (2020). Bi-allelic jam2 variants lead to early-onset recessive primary familial brain calcification. *The American Journal of Human Genetics* 106(3), 412–421.
- Sheng, W. and X. Yin (2013). Direction estimation in single-index models via distance covariance. *Journal of Multivariate Analysis* 122, 148–161.
- Sheng, W. and X. Yin (2016). Sufficient dimension reduction via distance covariance. *Journal of Computational and Graphical Statistics* 25(1), 91–104.
- Suzuki, T. (2019). Adaptivity of deep ReLU network for learning in Besov and mixed smooth Besov spaces: optimal rate and curse of dimensionality. In *International Conference on Learning Representations*.
- Suzuki, T. and A. Nitanda (2021). Deep learning is adaptive to intrinsic dimensionality of model smoothness in anisotropic besov space. *Advances in Neural Information Processing Systems* 34, 3609–3621.
- Székely, G. J. and M. L. Rizzo (2009). Brownian distance covariance. *Annals of Applied Statistics* 3(4), 1236–1265.
- Székely, G. J., M. L. Rizzo, and N. K. Bakirov (2007). Measuring and testing dependence by correlation of distances. *Annals of Statistics* 35(6), 2769 – 2794.
- Tian, Y. and Y. Feng (2023). Transfer learning under high-dimensional generalized linear models. *Journal of the American Statistical Association* 118(544), 2684–2697.
- Torrey, L. and J. Shavlik (2010). Transfer learning. In *Handbook of research on machine learning applications and trends: algorithms, methods, and techniques*, pp. 242–264. IGI global.
- Weiss, K., T. M. Khoshgoftaar, and D. Wang (2016). A survey of transfer learning. *Journal of Big data* 3, 1–40.
- Xu, K., L. Zhu, and J. Fan (2022). Distributed sufficient dimension reduction for heterogeneous massive data. *Statistica Sinica* 32, 2455–2476.
- Yang, T. and Q. Lin (2018). RSG: Beating subgradient method without smoothness and strong convexity. *Journal of Machine Learning Research* 19(6), 1–33.
- Zhu, L.-P., L.-X. Zhu, and Z.-H. Feng (2010). Dimension reduction in regressions through cumulative slicing estimation. *Journal of the American Statistical Association* 105(492), 1455–1466.
- Zhuang, F., Z. Qi, K. Duan, D. Xi, Y. Zhu, H. Zhu, H. Xiong, and Q. He (2020). A comprehensive survey on transfer learning. *Proceedings of the IEEE* 109(1), 43–76.

Appendix

The appendix contains additional technical details, further numerical results, and implementation specifications.

A Additional technical details

A.1 Anisotropic Besov Space Function Class

We now present the definition of the anisotropic Besov space (Suzuki and Nitanda, 2021, a-Besov). The a-Besov space is denoted as $B_{p,q,\tilde{\beta}}^{\beta}(\Omega)$ for $\beta = (\beta_1, \dots, \beta_d)^\top \in \mathbb{R}_{++}^d$ and $\tilde{\beta} = (\sum_{k=1}^d 1/\beta_k)^{-1}$. In this main text, we also use the abbreviation $B_{p,q,\tilde{\beta}}$ as the $\tilde{\beta}$ directly impact the final convergence analysis for the deep neural network estimator.

For function $f : [0, 1]^d \rightarrow \mathbb{R}$, we define the r th difference of f in the direction $h \in \mathbb{R}^d$ as

$$\Delta_h^r(f)(x) := \Delta_h^{r-1}(f)(x+h) - \Delta_h^{r-1}(f)(x), \Delta_h^0(f)(x) := f(x),$$

for $x, x+rh \in [0, 1]^d$, otherwise we set $\Delta_h^r(f)(x) = 0$.

Definition 1 For a function $f \in L^p(\Omega)$ where $p \in (0, \infty]$, the r -th modulus of smoothness of f is defined by $w_{r,p}(f, t) = \sup_{h \in \mathbb{R}^d: |h_i| \leq t_i} \|\Delta_h^r(f)\|_p$, for $t = (t_1, \dots, t_d)$, $t_i > 0$.

Definition 2 (Anisotropic Besov space $B_{p,q,\tilde{\beta}}^{\beta}(\Omega)$ (Suzuki and Nitanda, 2021)) For $0 < p, q \leq \infty$, $\beta = (\beta_1, \dots, \beta_d)^\top \in \mathbb{R}_{++}^d$, $r := \max_i \lfloor \beta_i \rfloor + 1$, let the semi-norm $|\cdot|_{B_{p,q,\tilde{\beta}}^{\beta}(\Omega)}$ be

$$|f|_{B_{p,q,\tilde{\beta}}^{\beta}(\Omega)} := \begin{cases} \left(\sum_{k=0}^{\infty} [2^k w_{r,p}(f, (2^{-k/\beta_1}, \dots, 2^{-k/\beta_d}))]^q \right)^{1/q} & (q < \infty), \\ \sup_{k \geq 0} 2^k w_{r,p}(f, (2^{-k/\beta_1}, \dots, 2^{-k/\beta_d})) & (q = \infty). \end{cases}$$

The norm of the anisotropic Besov space $B_{p,q,\tilde{\beta}}^{\beta}(\Omega)$ is defined by $\|f\|_{B_{p,q,\tilde{\beta}}^{\beta}(\Omega)} := \|f\|_p + |f|_{B_{p,q,\tilde{\beta}}^{\beta}(\Omega)}$ and the a-Besov space is defined as $B_{p,q,\tilde{\beta}}^{\beta}(\Omega) = \{f \in L^p(\Omega) : \|f\|_{B_{p,q,\tilde{\beta}}^{\beta}(\Omega)} < \infty\}$.

The a-Besov space can be used to avoid the curse of dimensionality and encompasses analyses of the Hölder space (Schmidt-hieber, 2020) and Besov space (Suzuki, 2019), as well as the low-dimensional manifold setting as special cases. We recall that the smoothness of the Hölder class or Sobolev class is defined by a scalar β , where the smoothness property is uniform across different directions. In contrast, $\beta \in \mathbb{R}^d$, the vector of smooth parameter for a-Besov class, represents the heterogeneous smoothness in each direction. An important quantity in the convergence analysis for a-Besov space is the average smoothness,

$$\tilde{\beta} = \left(\sum_{k=1}^d 1/\beta_k \right)^{-1}. \quad (\text{A.1})$$

We require that $\tilde{\beta}$ is large enough, i.e., $\tilde{\beta} > 1/p$, then functions are continuous. If β_i is large, then a function in $B_{p,q,\tilde{\beta}}^{\beta}(\Omega)$ is smooth to the i th coordinate direction, otherwise, it is non-smooth to that direction.

Again, we denote $B_{p,q,\tilde{\beta}}$ as an abbreviation of the a-Besov space in the main text as the $\tilde{\beta}$ directly impact the final convergence analysis for the deep neural network estimators.

A.2 Details of Linear Case

In the linear case presented in Section 3.4, the solutions B_c^* and B_t^* are typically non-unique. However, all solutions lead to the same central subspace (Ma and Zhu, 2013; Xu et al., 2022).

Here we study the projection matrix of B_c and B_t . For B_c ,

$$\mathbf{P}_{B_c} = \mathbf{X}B_c(B_c^\top \mathbf{X}^\top \mathbf{X}B_c)^{-1}B_c^\top \mathbf{X}^\top = \mathbf{X}B_cB_c^\top \mathbf{X}^\top,$$

where $(B_c^\top \mathbf{X}^\top \mathbf{X}B_c)^{-1} = I_{r_c}$ as $\mathbb{E}(\mathbf{X}) = \mathbf{0}$, $\text{Cov}(\mathbf{X}) = \mathbf{I}$ and $B_c^\top B_c = I_{r_c}$. Similarly, we have $\mathbf{P}_{B_t} = \mathbf{X}B_t(B_t^\top \mathbf{X}^\top \mathbf{X}B_t)^{-1}B_t^\top \mathbf{X}^\top = \mathbf{X}B_tB_t^\top \mathbf{X}^\top$. Then we obtain the projection matrix for $[B_c, B_t]$,

$$\begin{aligned} \mathbf{P}_{[B_c, B_t]} &= \mathbf{X} [B_c, B_t] \left(\begin{bmatrix} B_c^\top \\ B_t^\top \end{bmatrix} \mathbf{X}^\top \mathbf{X} [B_c, B_t] \right)^{-1} \begin{bmatrix} B_c^\top \\ B_t^\top \end{bmatrix} \mathbf{X}^\top \\ &= \mathbf{X} [B_c, B_t] \begin{bmatrix} B_c^\top \\ B_t^\top \end{bmatrix} \mathbf{X}^\top = \mathbf{X}B_cB_c^\top \mathbf{X}^\top + \mathbf{X}B_tB_t^\top \mathbf{X}^\top \\ &= \mathbf{P}_{B_c} + \mathbf{P}_{B_t}, \end{aligned} \tag{A.2}$$

where $B_c^\top B_t = 0$ and $\left(\begin{bmatrix} B_c^\top \\ B_t^\top \end{bmatrix} \mathbf{X}^\top \mathbf{X} [B_c, B_t] \right)^{-1} = \mathbf{I}$. It is clear that the space spanned by $[B_c, B_t]$ combines the information in both B_c and B_t .

We consider a simple example as follows,

$$\mathcal{D}_0 : Y \perp\!\!\!\perp X \mid [X_1, X_2, X_3, X_4]; \quad \mathcal{D}_1 : Y \perp\!\!\!\perp X \mid [X_1, X_2]; \quad \mathcal{D}_2 : Y \perp\!\!\!\perp X \mid [X_1, X_3],$$

where $\mathbb{E}(X) = \mathbf{0}$. $\text{Cov}(X) = \mathbf{I}$. Clearly, we have $\mathbf{P}_{B_c} = \mathbf{P}_{[X_1, X_2, X_3]}$, $\mathbf{P}_{B_t} = \mathbf{P}_{[X_4]}$ and $\mathbf{P}_{[B_c, B_t]} = \mathbf{P}_{B_c} + \mathbf{P}_{B_t}$. Then we have $[B_c, B_t]$ is a sufficient representation for the task on \mathcal{D}_0 where B_c and B_t draw the information of (X_1, X_2, X_3) and X_4 , respectively.

B Additional theoretical results and proofs

Below, C represents generic constants that may vary from line to line. The notation \mathcal{O} indicates the stochastic equivalent, while $\tilde{\mathcal{O}}$ denotes the stochastic equivalent up to some logarithmic factors.

B.1 Theoretical results for learning R_c

Recall $R_c^* = \text{argmin } \mathcal{L}_S(R)$ where

$$\mathcal{L}_S(R) = \sum_{s=1}^S \left\{ -\mathbb{V}(R(X_s), Y_s) + \lambda_E \mathbb{D}(R(X_s) \parallel \gamma_{r_c}) \right\} + \lambda_Z \mathbb{V}(R(X_{\text{pool}}), Z).$$

The empirical estimator \hat{R}_c is given as

$$\hat{R}_c = \text{argmin}_{R \in \mathcal{F}_{R_c}} \mathcal{L}_{S,n}(R),$$

where \mathcal{F}_{R_c} is the ReLU network class for learning R_c and

$$\mathcal{L}_{S,n}(R) = - \sum_{s=1}^S \left\{ \mathbb{V}_n(R(X_s), Y_s) + \lambda_E \mathbb{D}_n(R(X_s) || \gamma_r) \right\} + \lambda_Z \mathbb{V}_n(R(X_{pool}), Z_{pool}).$$

Under Assumption 1-3, set the tuning parameter $\lambda_E, \lambda_Z = \mathcal{O}(1)$, we have the excess risk bound for the \widehat{R}_c ,

$$\mathcal{L}_S(\widehat{R}_c) - \mathcal{L}_S(R_c^*) = \widetilde{\mathcal{O}}(\sqrt{r_c} N^{-\frac{\widehat{\beta}_c}{2\widehat{\beta}_c+1}}).$$

To obtain the result, we decompose the excess risk $\mathcal{L}_S(\widehat{R}_c) - \mathcal{L}_S(R_c^*)$ as follows,

$$\begin{aligned} \mathcal{L}_S(\widehat{R}_c) - \mathcal{L}_S(R_c^*) &= \mathcal{L}_S(\widehat{R}_c) - \mathcal{L}_{S,n}(\widehat{R}_c) \\ &\quad + \mathcal{L}_{S,n}(\widehat{R}_c) - \mathcal{L}_{S,n}(\widetilde{R}_c) \\ &\quad + \mathcal{L}_{S,n}(\widetilde{R}_c) - \mathcal{L}_S(\widetilde{R}_c) \\ &\quad + \mathcal{L}_S(\widetilde{R}_c) - \mathcal{L}_S(R_c^*), \end{aligned}$$

where $\widetilde{R}_c \in \mathcal{F}_{R_c}$ is any candidates from the neural network function class \mathcal{F}_{R_c} , R_c^* is the optimal sufficient and invariant representation.

The terms $\mathcal{L}_S(\widehat{R}_c) - \mathcal{L}_{S,n}(\widehat{R}_c)$ and $\mathcal{L}_{S,n}(\widetilde{R}_c) - \mathcal{L}_S(\widetilde{R}_c)$ can be bounded by the stochastic error $\sup_{R \in \mathcal{F}_{R_c}} |\mathcal{L}_S(R) - \mathcal{L}_{S,n}(R)|$. The term $\mathcal{L}_S(\widetilde{R}_c) - \mathcal{L}_S(R_c^*)$ depends on the approximation power of the neural network class \mathcal{F}_{R_c} . It can be controlled with $\inf_{\widetilde{R}_c \in \mathcal{F}_{R_c}} |\mathcal{L}_S(\widetilde{R}_c) - \mathcal{L}_S(R_c^*)|$ following the definition of \widetilde{R}_c . The term $\mathcal{L}_{S,n}(\widehat{R}_c) - \mathcal{L}_{S,n}(\widetilde{R}_c) \leq 0$ can be bounded by 0 in the inequality following the definition of \widehat{R}_c .

Thus we have

$$\mathcal{L}_S(\widehat{R}_c) - \mathcal{L}_S(R_c^*) < 2 \sup_{R \in \mathcal{F}_{R_c}} |\mathcal{L}_S(R) - \mathcal{L}_{S,n}(R)| + \inf_{\widetilde{R}_c \in \mathcal{F}_{R_c}} |\mathcal{L}_S(\widetilde{R}_c) - \mathcal{L}_S(R_c^*)|. \quad (\text{B.3})$$

B.1.1 Analysis for the approximation and the truncation error

In this section, we give the bound of

$$\inf_{\widetilde{R}_c \in \mathcal{F}_{R_c}} |\mathcal{L}_S(\widetilde{R}_c) - \mathcal{L}_S(R_c^*)|.$$

As the R_c^* follows the Gaussian distribution and is unbounded, we introduce its truncated version

$$T_B R(X) = \begin{cases} R(x), & \text{if } |R(x)| \leq B, \\ B, & \text{if } R(x) > B, \\ -B, & \text{if } R(x) < -B, \end{cases} \quad (\text{B.4})$$

where $B = \mathcal{O}(\log(N)^{1/2})$.

By the definition of \mathcal{L}_S ,

$$\begin{aligned}
|\mathcal{L}_S(\tilde{R}) - \mathcal{L}_S(R_c^*)| &< \sum_{s=1}^S |\mathbb{V}(\tilde{R}(X_s), Y_s) - \mathbb{V}(R_c^*(X_s), Y_s)| \\
&+ \lambda_E \sum_{s=1}^S |\mathbb{D}(\tilde{R}(X_s) || \gamma_{r_c}) - \mathbb{D}(R_c^*(X_s) || \gamma_{r_c})| \\
&+ \lambda_Z |\mathbb{V}(\tilde{R}(X_{pool}), Z_{pool}) - \mathbb{V}(R_c^*(X_{pool}), Z_{pool})|.
\end{aligned} \tag{B.5}$$

We analyze these terms one by one. For the first term $\mathbb{V}(\tilde{R}(X_s), Y_s) - \mathbb{V}(R_c^*(X_s), Y_s)$, with $s = 1, \dots, S$. We have

$$\begin{aligned}
&|\mathbb{V}(\tilde{R}(X_s), Y_s) - \mathbb{V}(R_c^*(X_s), Y_s)| \\
&= |\mathbb{V}(\tilde{R}(X_s), Y_s) - \mathbb{V}(T_B R_c^*(X_s), Y_s) + \mathbb{V}(T_B R_c^*(X_s), Y_s) - \mathbb{V}(R_c^*(X_s), Y_s)| \\
&< |\mathbb{V}(\tilde{R}(X_s), Y_s) - \mathbb{V}(T_B R_c^*(X_s), Y_s)| + |\mathbb{V}(T_B R_c^*(X_s), Y_s) - \mathbb{V}(R_c^*(X_s), Y_s)|.
\end{aligned} \tag{B.6}$$

Recall that $\mathbb{V}[z, y] = \mathbb{E}[\|z_1 - z_2\| \|y_1 - y_2\|] - 2\mathbb{E}[\|z_1 - z_2\| \|y_1 - y_3\|] + \mathbb{E}[\|z_1 - z_2\|] \mathbb{E}[\|y_1 - y_2\|]$, where $(z_i, y_i), i = 1, 2, 3$ are i.i.d. copies of (z, y) (Székely et al., 2007). We have

$$\begin{aligned}
&|\mathbb{V}[T_B R_c^*(x), y] - \mathbb{V}[\tilde{R}(x), y]| \\
&\leq \left| \mathbb{E} \left[(\|T_B R_c^*(x_1) - T_B R_c^*(x_2)\| - \|\tilde{R}(x_1) - \tilde{R}(x_2)\|) |y_1 - y_2| \right] \right| \\
&+ 2 \left| \mathbb{E} \left[(\|T_B R_c^*(x_1) - T_B R_c^*(x_2)\| - \|\tilde{R}(x_1) - \tilde{R}(x_2)\|) |y_1 - y_3| \right] \right| \\
&+ \left| \mathbb{E} \left[\|T_B R_c^*(x_1) - T_B R_c^*(x_2)\| - \|\tilde{R}(x_1) - \tilde{R}(x_2)\| \right] \mathbb{E} \left[\|y_1 - y_2\| \right] \right| \\
&\leq 8C \mathbb{E} \left[\left| \|T_B R_c^*(x_1) - T_B R_c^*(x_2)\| - \|\tilde{R}(x_1) - \tilde{R}(x_2)\| \right| \right] \\
&\leq 16C \mathbb{E} \|T_B R_c^*(x) - \tilde{R}(x)\|.
\end{aligned} \tag{B.7}$$

The first and third inequalities follow the triangle inequality. The second inequality holds due to the boundedness of y .

Similarly,

$$|\mathbb{V}(T_B R_c^*(X_s), Y_s) - \mathbb{V}(R_c^*(X_s), Y_s)| < 16C \mathbb{E} \|T_B R_c^*(x) - R_c^*(x)\|.$$

For $1 \leq i \leq d$, denote $R_{c,k}^*$ as the k -th element of R_c^* and $B = \mathcal{O}(\log(N)^{1/2})$,

$$\mathbb{E} |R_{c,k}^* - T_B R_{c,k}^*| = 2 \int_B^\infty \frac{x}{\sqrt{2\pi}} e^{-x^2/2} dx = \frac{-2e^{-x^2/2}}{\sqrt{2\pi}} \Big|_B^\infty = \frac{2e^{-B^2/2}}{\sqrt{2\pi}} = \mathcal{O}(N^{-1}). \tag{B.8}$$

In conclusion,

$$|\mathbb{V}(\tilde{R}(X_s), Y_s) - \mathbb{V}(R_c^*(X_s), Y_s)| = \mathcal{O}(\mathbb{E} \|T_B R_c^*(x) - \tilde{R}(x)\|) + \mathcal{O}(N^{-1}), \tag{B.9}$$

with $B = \mathcal{O}(\log(N)^{1/2})$.

For the second term, it is similar that we have

$$\left| \mathbb{V}[\tilde{R}(x), Z_{pool}] - \mathbb{V}[R_c^*(x), Z_{pool}] \right| \leq 16C\mathbb{E}\|\tilde{R}(x) - R_c^*(x)\| + \mathcal{O}(N^{-1}). \quad (\text{B.10})$$

For the third term $|\mathbb{D}(\tilde{R}(X_s)|\gamma_{r_c}) - \mathbb{D}(R_c^*(X_s)|\gamma_{r_c})|$, for $s = 1, \dots, S$. Obviously we have $\mathbb{D}(R_c^*(X_s)|\gamma_{r_c}) = 0$ given R_c^* follows the standard Gaussian distribution. Recall that $\mathbb{D}(X|\gamma_{r_c}) = \mathbb{D}(X, U)$ where $U \sim N(0, I_{r_c})$ is the independently generated random samples.

$$\begin{aligned} & |\mathbb{D}(\tilde{R}(X_s), U) - \mathbb{D}(R^*(X_s), U)| \\ &= |\mathbb{D}(\tilde{R}(X_s), U) - \mathbb{D}(T_B R^*(X_s), U) + \mathbb{D}(T_B R^*(X_s), U) - \mathbb{D}(R^*(X_s), U)| \\ &\leq |\mathbb{D}(\tilde{R}(X_s), U) - \mathbb{D}(T_B R^*(X_s), U)| + |\mathbb{D}(T_B R^*(X_s), U) - \mathbb{D}(R^*(X_s), U)| \end{aligned} \quad (\text{B.11})$$

For the first term in (B.11),

$$\begin{aligned} & |\mathbb{D}(\tilde{R}(X_s), U) - \mathbb{D}(T_B R^*(X_s), U)| \\ &\leq 2|E\|\tilde{R}(X) - U\| - E\|T_B R^*(X) - U\|| \\ &+ |E\|\tilde{R}(X_1) - \tilde{R}(X_2)\| - E\|T_B R^*(X_1) - T_B R^*(X_2)\|| \\ &+ |E\|U_1 - U_2\| - E\|U_1 - U_2\|| \\ &\leq 4E\|\tilde{R}(X) - T_B R^*(X)\|. \end{aligned} \quad (\text{B.12})$$

The last inequality holds following the triangular inequality. Similarly, for the second term in (B.11),

$$|\mathbb{D}(T_B R^*(X_s), U) - \mathbb{D}(R^*(X_s), U)| \leq 4E\|T_B R^*(X) - R^*(X)\| = \mathcal{O}(N^{-1}). \quad (\text{B.13})$$

The last equality follows result (B.8) and $B = \mathcal{O}(\log(N)^{1/2})$.

Combining the results (B.7), (B.10), (B.12), (B.13), we have that

$$\inf_{\tilde{R} \in \mathcal{F}} |\mathcal{L}_S(\tilde{R}_c) - \mathcal{L}_S(R_c^*)| = \mathcal{O}\left(E\|\tilde{R}(X) - T_B R_c^*(X)\|\right) + \mathcal{O}(N^{-1}). \quad (\text{B.14})$$

Actually the first term is the approximation error for neural network class in learning functions and the second term is the truncated error.

Then we derive the bound for the term

$$\mathbb{E}\|\tilde{R}(X) - T_B R_c^*(X)\|.$$

It suffices to control the $\|\tilde{R}(X) - T_B R_c^*(X)\|_{L^\infty}$. For the i -th element of the \tilde{R} and $T_B R_c^*$, we have

$$\begin{aligned} \|T_B R_{c,i}^* - \tilde{R}_i\|_{L^2(\mu_x)} &= \left[\int (T_B R_{c,i}^*(x) - \tilde{R}_i(x))^2 f_X(x) dx \right]^{1/2} \\ &\leq \|T_B R_{c,i}^* - \tilde{R}_i\|_{L^\infty} \int f_X(x) dx \\ &\leq C \|T_B R_{c,i}^* - \tilde{R}_i\|_{L^\infty}. \end{aligned}$$

Lemma B.1 Recall that $R_c^* = (R_{c,1}^*, \dots, R_{c,r_c}^*)$ where $R_{c,i}^* \in B_{p,q,\tilde{\beta}_{c,i}}(\Omega)$ for $i = 1, \dots, r_c$. Here exists $\tilde{R}_{c,i} \in \mathcal{F}_{R_c}$ where the \mathcal{F}_{R_c} satisfying the Assumption 2 in the main text, we have that

$$\|\tilde{R}_{c,i} - T_B R_{c,i}^*\|_{L^\infty} \leq \tilde{\mathcal{O}}(N^{\tilde{\beta}_c/(2\tilde{\beta}_c+1)}), \quad (\text{B.15})$$

where $\tilde{\beta}_c = \min\{\tilde{\beta}_{c,1}, \dots, \tilde{\beta}_{c,r_c}\}$, $N = \sum_{s=1}^S n_s$ and $N = \mathcal{O}(n_s)$ as S is finite.

Proof 1 This Lemma follows directly Proposition 2 of Suzuki and Nitanda (2021).

Then we have

$$\begin{aligned} \|\tilde{R}_c - R_c\|_{L^\infty} &\leq \tilde{\mathcal{O}}(\sqrt{r_c} N^{\tilde{\beta}_c/(2\tilde{\beta}_c+1)}), \\ \inf_{R \in \mathcal{F}_{R_c}} |\mathcal{L}_S(\tilde{R}_c) - \mathcal{L}_S(R_c^*)| &\leq \tilde{\mathcal{O}}(\sqrt{r_c} N^{\tilde{\beta}_c/(2\tilde{\beta}_c+1)}). \end{aligned} \quad (\text{B.16})$$

B.1.2 Analysis for the stochastic error

In this section, we bound the stochastic error $\sup_{R \in \mathcal{F}_{R_c}} |\mathcal{L}_{S,n}(R) - \mathcal{L}_S(R)|$.

We have

$$\begin{aligned} \sup_{R \in \mathcal{F}_{R_c}} |\mathcal{L}_{S,n}(R) - \mathcal{L}_S(R)| &\leq \sup_{R \in \mathcal{F}_{R_c}} \sum_{s=1}^S \left| \mathbb{V}_n(R(X_s), Y_s) - \mathbb{V}(R(X_s), Y_s) \right| \\ &\quad + \sup_{R \in \mathcal{F}_{R_c}} \sum_{s=1}^S \left| \mathbb{D}_n(R(X_s) || \gamma_{r_c}) - \mathbb{D}(R(X_s) || \gamma_{r_c}) \right| \\ &\quad + \sup_{R \in \mathcal{F}_{R_c}} \left| \mathbb{V}_n(R(X_{pool}), Z_{pool}) - \mathbb{V}(R(X_{pool}), Z_{pool}) \right|. \end{aligned} \quad (\text{B.17})$$

In the present problem, the objective function is the combination of loss functions with U -process type indexed by a class of neural networks.

First we consider the first term of (B.17),

$$\begin{aligned} \sup_{R \in \mathcal{F}_{R_c}} \sum_{s=1}^S \left| \mathbb{V}_n(R(X_s), Y_s) - \mathbb{V}(R(X_s), Y_s) \right| \\ \leq \sum_{s=1}^S \sup_{R \in \mathcal{F}_{R_c}} \left| \mathbb{V}_n(R(X_s), Y_s) - \mathbb{V}(R(X_s), Y_s) \right| \\ \leq CS \sup_{R \in \mathcal{F}_{R_c}} \left| \mathbb{V}_n(R(X_1), Y_1) - \mathbb{V}(R(X_1), Y_1) \right|. \end{aligned}$$

where S is the number of sources and C is some constant. It suffice for us to bound the stochastic error

$$\sup_{R \in \mathcal{F}_{R_c}} \left| \mathbb{V}_n(R(X_1), Y_1) - \mathbb{V}(R(X_1), Y_1) \right|.$$

Denote $\forall R \in \mathcal{F}_{R_c}$ where \mathcal{F}_{R_c} is the class of neural networks. Let $\tilde{\mathcal{O}} = (R(x), y)$ denotes the random variables from the domain $s = 1$ and we omit the source subscript here for simplicity.

We denote $\tilde{O}_i = (R(x_i), y_i), i = 1, \dots, n_1$ are i.i.d copy of \tilde{O} . We define centered kernel as

$$\begin{aligned} \bar{h}_R(\tilde{O}_1, \tilde{O}_2, \tilde{O}_3, \tilde{O}_4) &= \frac{1}{4} \sum_{\substack{1 \leq i, j \leq 4, \\ i \neq j}} \|R(x_i) - R(x_j)\| |y_i - y_j| \\ &- \frac{1}{4} \sum_{i=1}^4 \left(\sum_{\substack{1 \leq j \leq 4, \\ j \neq i}} \|R(x_i) - R(x_j)\| \sum_{\substack{1 \leq j \leq 4, \\ i \neq j}} |y_i - y_j| \right) \\ &+ \frac{1}{24} \sum_{\substack{1 \leq i, j \leq 4, \\ i \neq j}} \|R(x_i) - R(x_j)\| \sum_{\substack{1 \leq i, j \leq 4, \\ i \neq j}} |y_i - y_j| - \mathbb{V}[R(x), y]. \end{aligned} \quad (\text{B.18})$$

Then, the centered U -statistics $\mathbb{U}_n(R(X), Y) - \mathbb{V}(R(X), Y)$ can be expressed as

$$\mathbb{U}_{n_1}(\bar{h}_R) = \frac{1}{\binom{n_1}{4}} \sum_{i_1 < i_2 < i_3 < i_4} \bar{h}_R(\tilde{O}_{i_1}, \tilde{O}_{i_2}, \tilde{O}_{i_3}, \tilde{O}_{i_4}).$$

By the symmetrization randomization (Theorem 3.5.3 in De la Pena and Giné (2012)), we have

$$\mathbb{E} \left[\sup_{R \in \mathcal{F}_{R_c}} |\mathbb{U}_{n_1}(\bar{h}_R)| \right] \leq C \mathbb{E} \left[\sup_{R \in \mathcal{F}_{R_c}} \left| \frac{1}{\binom{n_1}{4}} \sum_{1 \leq i_1 < i_2 < i_3 < i_4 \leq n} \epsilon_{i_1} \bar{h}_R(\tilde{O}_{i_1}, \tilde{O}_{i_2}, \tilde{O}_{i_3}, \tilde{O}_{i_4}) \right| \right], \quad (\text{B.19})$$

where, $\epsilon_{i_1}, i_1 = 1, \dots, n_1$ are i.i.d Rademacher variables that are also independent with $\tilde{O}_i, i = 1, \dots, n_1$.

We then bound the above Rademacher process with the metric entropy of the neural network class \mathcal{F}_{R_c} . Recall that under Assumption 1, the kernel \bar{h}_R is also bounded for $R \in \mathcal{F}_{R_c}$. $\forall R \in \mathcal{F}_{R_c}$, we define a random empirical measure for the pair (R, R_δ) ,

$$e_{n_1,1}(R, R_\delta) = \mathbb{E}_{\epsilon_{i_1}, i_1=1, \dots, n_1} \left| \frac{1}{\binom{n_1}{4}} \sum_{i_1 < i_2 < i_3 < i_4} \epsilon_{i_1} (\bar{h}_R - \bar{h}_{R_\delta})(\tilde{O}_{i_1}, \dots, \tilde{O}_{i_4}) \right|.$$

Condition on $\{X_i, Y_i\}_{i=1, \dots, n_1}$, let $\mathcal{N}(\mathcal{F}_{R_c}, e_{n_1,1}, \delta)$ be the covering number of the neural network class \mathcal{F}_{R_c} with respect to the empirical distance $e_{n_1,1}$ at scale of $\delta > 0$. Denote \mathcal{F}_δ as the covering set of \mathcal{F}_{R_c} with cardinality of $\mathcal{N}(\mathcal{F}_{R_c}, e_{n_1,1}, \delta)$. Then,

$$\begin{aligned} &\mathbb{E}_{\epsilon_{i_1}} \left[\sup_{R \in \mathcal{F}_{R_c}} \left| \frac{1}{\binom{n_1}{4}} \sum_{i_1 < i_2 < i_3 < i_4} \epsilon_{i_1} \bar{h}_R(\tilde{O}_{i_1}, \tilde{O}_{i_2}, \tilde{O}_{i_3}, \tilde{O}_{i_4}) \right| \right] \\ &\leq \delta + \mathbb{E}_{\epsilon_{i_1}} \left[\sup_{R \in \mathcal{F}_\delta} \left| \frac{1}{\binom{n_1}{4}} \sum_{i_1 < i_2 < i_3 < i_4} \epsilon_{i_1} \bar{h}_R(\tilde{O}_{i_1}, \tilde{O}_{i_2}, \tilde{O}_{i_3}, \tilde{O}_{i_4}) \right| \right] \\ &\leq \delta + C \frac{1}{\binom{n_1}{4}} (\log \mathcal{N}(\mathcal{F}_{R_c}, e_{n_1,1}, \delta))^{1/2} \max_{R \in \mathcal{F}_\delta} \left[\sum_{i_1=1}^{n_1} \left(\sum_{i_2 < i_3 < i_4} \bar{h}_R(\tilde{O}_{i_1}, \tilde{O}_{i_2}, \tilde{O}_{i_3}, \tilde{O}_{i_4}) \right)^2 \right]^{1/2} \\ &\leq \delta + C \mathcal{B} (\log \mathcal{N}(\mathcal{F}_{R_c}, e_{n_1,1}, \delta))^{1/2} \frac{1}{\binom{n_1}{4}} \left[\frac{n_1 (n_1!)^2}{((n_1 - 3)!)^2} \right]^{1/2} \\ &\leq \delta + 2C \mathcal{B} (\log \mathcal{N}(\mathcal{F}_{R_c}, e_{n_1,1}, \delta))^{1/2} / \sqrt{n_1}. \end{aligned}$$

Where \mathcal{B} is the upper bound of the weights in the neural network class. The third inequality follows the Lemma 8.8 of Huang et al. (2024). Thus the stochastic error can be bounded

with the sample size n_1 , the pre-given covering scale δ and the corresponding covering number $\mathcal{N}(\mathcal{F}_{R_c}, e_{n_1,1}, \delta)$.

We mention that here we learn R_c with dimension r_c . In the Assumption 3, we consider that the width of the network $\mathcal{F}_{r_c} : \mathbb{R}^d \rightarrow \mathbb{R}^{r_c}$ is linear with r_c , ensuring the expression power for learning the R of dimension r_c . We have the result that $\mathcal{N}(\mathcal{F}_{R_c}, e_{n_1,1}, \delta) < \mathcal{N}^{r_c}(\mathcal{F}_1, e_{n_1,1}, \delta)$, where \mathcal{F}_1 is the neural network class with output of dimension 1, the depth $\mathcal{H}_{\mathcal{F}_1} = \mathcal{O}(\log(d) \log(N))$, width $\mathcal{W}_{\mathcal{F}_1} = \mathcal{O}(dN^{1/(2\tilde{\beta}_c+1)})$ and model size $\mathcal{S}_{\mathcal{F}_1} = \mathcal{O}(d^2 N^{1/(2\tilde{\beta}_c+1)} \log(N) \log(d))$. The size of the covering set of \mathcal{F}_{R_c} can be bounded as the product of the size of the covering set of \mathcal{F}_1 .

With the result $\mathcal{N}(\mathcal{F}_1, e_{n_1,1}, \delta) < \mathcal{N}(\mathcal{F}_1, e_{n_1,\infty}, \delta)$ and the relationship between the metric entropy and the VC-dimension of \mathcal{F} , we have (Anthony and Bartlett, 2009),

$$\log \mathcal{N}(\mathcal{F}_1, e_{n_1,\infty}, \delta) \leq \text{VC}_{\mathcal{F}_1} \log \frac{2en_1\mathcal{B}}{\delta \text{VC}_{\mathcal{F}_1}}.$$

Following the result of Bartlett et al. (2019), the $\text{VC}_{\mathcal{F}_1}$ can be bounded by the depth, width and the number of parameters of the ReLU network,

$$c\mathcal{H}_{\mathcal{F}_1}\mathcal{S}_{\mathcal{F}_1} \log \mathcal{S}_{\mathcal{F}_1} \leq \text{VC}_{\mathcal{F}_1} \leq C\mathcal{H}_{\mathcal{F}_1}\mathcal{S}_{\mathcal{F}_1} \log \mathcal{S}_{\mathcal{F}_1}, \quad (\text{B.20})$$

where c, C are two different constant.

Thus we have

$$\begin{aligned} & \mathbb{E}_{\epsilon_{i_1}} \left[\sup_{R \in \mathcal{F}_{R_c}} \left| \frac{1}{\binom{n_1}{4}} \sum_{i_1 < i_2 < i_3 < i_4} \epsilon_{i_1} \bar{h}_R(\tilde{O}_{i_1}, \tilde{O}_{i_2}, \tilde{O}_{i_3}, \tilde{O}_{i_4}) \right| \right] \\ & \leq \delta + 2C\mathcal{B}(r_c \log \mathcal{N}(\mathcal{F}_1, e_{n_1,1}, \delta))^{1/2} / \sqrt{n_1} \\ & \leq \delta + C\mathcal{B}(r_c \mathcal{H}_{\mathcal{F}_1} \mathcal{S}_{\mathcal{F}_1} \log \mathcal{S}_{\mathcal{F}_1} \log \frac{\mathcal{B}n_1}{\delta \mathcal{H}_{\mathcal{F}_1} \mathcal{S}_{\mathcal{F}_1} \log \mathcal{S}_{\mathcal{F}_1}})^{1/2} / \sqrt{n_1} \\ & \leq \tilde{\mathcal{O}}(\sqrt{r_c n_1^{-\frac{\tilde{\beta}}{2\tilde{\beta}+1}}}) + \frac{1}{n_1}. \end{aligned} \quad (\text{B.21})$$

The last line holds with setting $\delta = 1/n_1$ and Assumption 3 for the DNN structure. In conclusion,

$$\begin{aligned} & \sup_{R \in \mathcal{F}_{R_c}} \sum_{s=1}^S |\mathbb{V}(R(X_s), Y_s) - \mathbb{V}_n(R(X_s), Y_s)| \\ & \lesssim CS \sup_{R \in \mathcal{F}_{R_c}} |\mathbb{V}(R(X_1), Y_1) - \mathbb{V}_n(R(X_1), Y_1)| \\ & \leq \tilde{\mathcal{O}}(\sqrt{r_c n_1^{-\frac{\tilde{\beta}}{2\tilde{\beta}+1}}}) = \tilde{\mathcal{O}}(\sqrt{r_c N^{-\frac{\tilde{\beta}}{2\tilde{\beta}+1}}}). \end{aligned} \quad (\text{B.22})$$

The last equality holds as S , the number of sources, is finite and $N = \mathcal{O}(n_s)$ for $s = 1, \dots, S$.

For the second term of (B.17), we have

$$\sup_{R \in \mathcal{F}_{R_c}} |\mathbb{V}(R(X_{pool}), Z_{pool}) - \mathbb{V}_n(R(X_{pool}), Z_{pool})| \leq \tilde{\mathcal{O}}(\sqrt{r_c N^{-\frac{\tilde{\beta}}{2\tilde{\beta}+1}}}). \quad (\text{B.23})$$

The result can be obtained similarly as that for the first term of (B.17).

For the third term of (B.17), we have

$$\begin{aligned} \sup_{R \in \mathcal{F}_{R_c}} \sum_{s=1}^S \left| \mathbb{D}(R(X_s) | \gamma_{r_c}) - \mathbb{D}_n(R(X_s) | \gamma_{r_c}) \right| &\leq \sum_{s=1}^S \sup_{R \in \mathcal{F}_{R_c}} \left| \mathbb{D}(R(X_s) | \gamma_{r_c}) - \mathbb{D}_n(R(X_s) | \gamma_{r_c}) \right| \\ &\leq CS \sup_{R \in \mathcal{F}_{R_c}} \left| \mathbb{D}(R(X_s) | \gamma_{r_c}) - \mathbb{D}_n(R(X_s) | \gamma_{r_c}) \right|. \end{aligned} \quad (\text{B.24})$$

It suffices to bound the term $\sup_{R \in \mathcal{F}} \left| \mathbb{D}(R(X_s), U) - \mathbb{D}_n(R(X_s), U) \right|$ where the $U \sim N(0, I_{r_c})$ is drawn from the standard Gaussian distribution and

$$\tilde{\mathbb{D}}_n(R(X), Y) = \frac{1}{\binom{n}{2}} \sum_{1 \leq i, j \leq n} h_e(\tilde{O}_i; \tilde{O}_j),$$

where $h_e(\tilde{O}_i; \tilde{O}_j) = h_e(u_1, u_2; v_1, v_2) = \|u_1 - v_2\| + \|u_2 - v_1\| - \|u_1 - u_2\| - \|v_1 - v_2\|$ (Gretton et al., 2012). The $\tilde{O}_i = (R(x_i), y_i), i = 1, \dots, n_1$ is defined before the expression (B.18). Thus we can also construct the following centered kernel

$$\begin{aligned} \bar{h}_e(\tilde{O}_i, \tilde{O}_j) := &\|R(x_i) - U_i\| + \|R(x_j) - U_j\| - \|R(x_i) - R(x_j)\| - \|U_i - U_j\| \\ &- \mathbb{D}(R(x), U). \end{aligned}$$

Thus the centered U-statistics $\mathbb{D}_n - \mathbb{D}$ can be expressed as

$$\mathbb{U}_{e,n} = \frac{1}{\binom{n}{2}} \sum_{1 \leq i_1 < i_2 \leq n} \bar{h}_e(\tilde{O}_{i_1}, \tilde{O}_{i_2}).$$

By the symmetrization randomization, we have

$$\mathbb{E} \left[\sup_{R \in \mathcal{F}_{R_c}} \mathbb{U}_{e,n}(\bar{h}_e) \right] \leq C \mathbb{E} \left[\sup_{R \in \mathcal{F}_{R_c}} \frac{1}{\binom{n_1}{2}} \sum_{i_1 < i_2} \epsilon_{i_1} \bar{h}_e(\tilde{O}_{i_1}, \tilde{O}_{i_2}) \right],$$

where ϵ_{i_1} is the Rademacher variables corresponding for the decoupling.

Define

$$\tilde{e}_{n,1}(R, R_\delta) = \mathbb{E}_{\epsilon_i, i=1, \dots, n} \left| \frac{1}{\binom{n}{2}} \sum_{1 \leq i_1 < i_2 \leq n} \epsilon_i (\bar{h}_R - \bar{h}_{R_\delta})(\tilde{O}_{i_1}, \tilde{O}_{i_2}) \right|.$$

Condition on $\{X_i, Y_i\}_{i=1, \dots, n_1}$, let $\mathcal{N}(\mathcal{F}_{R_c}, \tilde{e}_{n,1}, \delta)$ be the covering number of the neural network class \mathcal{F}_{R_c} with respect to the empirical distance $\tilde{e}_{n,1}$ at scale of $\delta > 0$. Denote $\mathcal{F}_{\delta, \tilde{e}}$ as the covering set of \mathcal{F} with cardinality of $\mathcal{N}(\mathcal{F}_{R_c}, \tilde{e}_{n,1}, \delta)$.

Then,

$$\begin{aligned}
& \mathbb{E}_{\epsilon_{i_1}} \left[\sup_{R \in \mathcal{F}_{R_c}} \left| \frac{1}{\binom{n_1}{2}} \sum_{i_1 < i_2} \epsilon_{i_1} \bar{h}_e(\tilde{O}_{i_1}, \tilde{O}_{i_2}) \right| \right] \\
& \leq \delta + \mathbb{E}_{\epsilon_{i_1}} \left[\sup_{R \in \mathcal{F}_\delta} \left| \frac{1}{\binom{n_1}{2}} \sum_{i_1 < i_2} \epsilon_{i_1} \bar{h}_R(\tilde{O}_{i_1}, \tilde{O}_{i_2}) \right| \right] \\
& \leq \delta + C(\log \mathcal{N}(\mathcal{F}_{R_c}, \tilde{e}_{n_1,1}, \delta))^{1/2} \frac{1}{\binom{n_1}{2}} \max_{R \in \mathcal{F}_\delta} \left[\sum_{i_1=1}^{n_1} \left(\sum_{i_2} \bar{h}_R(\tilde{O}_{i_1}, \tilde{O}_{i_2}) \right)^2 \right]^{1/2} \\
& \leq \delta + 2C\mathcal{B}(\log \mathcal{N}(\mathcal{F}_{R_c}, \tilde{e}_{n_1,1}, \delta))^{1/2} \frac{2}{n_1(n_1-1)} \left[\sum_{i=1}^{n_1} Cn_1^2 \right]^{1/2} \\
& \leq \delta + 2C\mathcal{B}(\log \mathcal{N}(\mathcal{F}_{R_c}, \tilde{e}_{n_1,1}, \delta))^{1/2} / \sqrt{n_1} \\
& \leq \tilde{\mathcal{O}}(\sqrt{r_c} n_1^{-\frac{\tilde{\beta}}{2\tilde{\beta}+1}}) + \frac{1}{n_1}.
\end{aligned}$$

The last inequality follows the result of (B.21).

Thus we have

$$\sup_{R \in \mathcal{F}_{R_c}} \sum_{s=1}^S |\mathbb{D}(R(X_s) \parallel \gamma_r) - \mathbb{D}_n(R(X_s) \parallel \gamma_{r_c})| \leq \tilde{\mathcal{O}}(\sqrt{r_c} n_1^{-\frac{\tilde{\beta}}{2\tilde{\beta}+1}}) = \tilde{\mathcal{O}}(\sqrt{r_c} N^{-\frac{\tilde{\beta}}{2\tilde{\beta}+1}}). \quad (\text{B.25})$$

Combining (B.16), (B.22), (B.23), (B.25), we have the excess risk bound for the \hat{R}_c and the R_c^* ,

$$\begin{aligned}
\mathcal{L}_S(\hat{R}_c) - \mathcal{L}_S(R_c^*) & < 2 \sup_{R \in \mathcal{F}_{R_c}} |\mathcal{L}_S(R) - \mathcal{L}_{S,n}(R)| + \inf_{R \in \mathcal{F}_{R_c}} |\mathcal{L}_S(R) - \mathcal{L}_S(R_c^*)| \\
& \leq \tilde{\mathcal{O}}(\sqrt{r_c} N^{-\frac{\tilde{\beta}}{2\tilde{\beta}+1}}).
\end{aligned} \quad (\text{B.26})$$

We mention that the optimal solution for SIRep is non-unique but the existence of such $R_c \in \mathcal{M}_{R_c}$ is ensured where $\mathcal{M}_{R_c} = \{R_c : \mathbb{R}^d \rightarrow \mathbb{R}^{r_c}, Y_s \perp\!\!\!\perp X_s \mid R(X_s), \text{ for } s = 1, \dots, S, R_c(X) \sim N(\mathbf{0}, \mathbf{I}_{r_c}) \text{ and } R_c(X) \perp\!\!\!\perp Z\}$ (Lee et al., 2013; Chen et al., 2024). Following the idea of Zhu et al. (2010); Sheng and Yin (2016), we study the the distance between the \hat{R} and R_c^* where R_c^* is one of the global optimal points such that \hat{R}_c converges to R_c^* .

Following Yang and Lin (2018), given R_c^* and the local set $\mathcal{M}_\rho(R_c^*)$ where $\mathcal{M}_\rho(R_c^*) = \{R'_c : \|R_c^* - R'_c\| \leq \rho, \text{ and } R'_c \sim N(0, 1)\}$, we have for $R'_c \in \mathcal{M}_\rho(R_c^*)$,

$$\|R'_c - R_c^*\|_2^2 \leq C |\mathbb{V}(R_c^*, y) - \mathbb{V}(R'_c, y)|. \quad (\text{B.27})$$

Without loss of generality, we prove the result considering the case for $R : \mathbb{R}^d \rightarrow \mathbb{R}^r$ with $r = 1$. As $R'_c \sim N(0, 1)$ and $R'_c \in \mathcal{M}_\rho$, we have the following expression, $R'_c = (1 - \rho)R_c^* + \epsilon$ where ρ is the correlation coefficient and $\epsilon \sim N(0, 2\rho - \rho^2)$. First we have

$$\begin{aligned}
\|R'_c - R_c^*\|_{L_2(P(X))}^2 & = (\rho R_c^* + \epsilon)^2 = \rho^2 \text{Var}(R_c^*) + \text{Var}(\epsilon) \\
& = \rho^2 + 2\rho - \rho^2 = 2\rho.
\end{aligned}$$

Asymptotically, we have $\rho \rightarrow 0$ and thus $\|R'_c - R_c^*\| = \mathcal{O}(\rho^{1/2}) \rightarrow 0$. Then, by Theorem 3 of Székely and Rizzo (2009),

$$\mathbb{V}(R'_c, y) = \mathbb{V}[(1 - \rho)R_c^* + \epsilon, y] \leq (1 - \rho)\mathbb{V}[R_c^*, y] + \mathbb{V}[\epsilon, 0] \leq (1 - \rho)\mathbb{V}[R_c^*, y].$$

Thus we have $\mathbb{V}(R_c^*, y) - \mathbb{V}(R'_c, y) > \rho\mathbb{V}(R_c^*, y) > \rho C$. $\mathbb{V}(R_c^*, y) > C$ is natural as the sufficient and invariance representation R_c^* has prediction power for y thus the distance covariance is bounded away from 0. Thus $\|R'_c - R_c^*\|_2^2 \leq 2C|\mathbb{V}(R_c^*, y) - \mathbb{V}(R'_c, y)|$ holds. Then we have

$$\|\widehat{R}_c - R_c^*\| \leq \widetilde{\mathcal{O}}(r_c^{1/4} n_s^{-\frac{\tilde{\beta}_c/2}{2\tilde{\beta}_c+1}}). \quad (\text{B.28})$$

B.2 Theoretical results for learning R_t .

Recall that

$$\mathcal{L}_T([R_t, R_c]) = -\mathbb{V}([R_t(X_0), R_c(X_0)], Y_0) + \lambda_{E,0}\mathbb{D}(R_t(X_0)|\gamma_{r_t}) + \lambda_C\mathbb{V}(R_t(X_0), R_c(X_0)),$$

and its empirical counterpart is

$$\mathcal{L}_{T,n}([R_t, R_c]) = -\mathbb{V}_n([R_t(X_0), R_c(X_0)], Y_0) + \lambda_{E,0}\mathbb{D}_n(R_t(X_0)|\gamma_{r_t}) + \lambda_C\mathbb{V}_n(R_t(X_0), R_c(X_0)),$$

where the tuning parameters $\lambda_{E,0}, \lambda_C = \mathcal{O}(1)$, $\mathbb{V}_n, \mathbb{D}_n$ are the empirical version of \mathbb{V}, \mathbb{D} , respectively.

The excess risk of $[\widehat{R}_t, \widehat{R}_c]$ can be decomposed as follows,

$$\begin{aligned} \mathcal{L}_T([\widehat{R}_t, \widehat{R}_c]) - \mathcal{L}_T([R_t^*, R_c^*]) &= -\mathbb{V}([\widehat{R}_t(X_0), \widehat{R}_c(X_0)], Y_0) + \mathbb{V}([R_t^*(X_0), R_c^*(X_0)], Y_0) \\ &\quad + \lambda_C\mathbb{V}(\widehat{R}_t(X_0), \widehat{R}_c(X_0)) - \lambda_C\mathbb{V}(R_t^*(X_0), R_c^*(X_0)) \\ &\quad + \lambda_{E,0}\mathbb{D}(\widehat{R}_t(X_0)|\gamma_{r_t}) - \lambda_{E,0}\mathbb{D}(R_t^*(X_0)|\gamma_{r_t}) \\ &= I + II + III. \end{aligned} \quad (\text{B.29})$$

For the term I ,

$$\begin{aligned} I &= \mathbb{V}([R_t^*(X_0), R_c^*(X_0)], Y_0) - \mathbb{V}([\widehat{R}_t(X_0), \widehat{R}_c(X_0)], Y_0) \\ &= \mathbb{V}([R_t^*(X_0), R_c^*(X_0)], Y_0) - \mathbb{V}([\widehat{R}_t(X_0), R_c^*(X_0)], Y_0) \\ &\quad + \mathbb{V}([\widehat{R}_t(X_0), R_c^*(X_0)], Y_0) - \mathbb{V}([\widehat{R}_t(X_0), \widehat{R}_c(X_0)], Y_0) \end{aligned} \quad (\text{B.30})$$

For the second part of (B.30), we have,

$$\begin{aligned} &\mathbb{V}([\widehat{R}_t(X_0), R_c^*(X_0)], Y_0) - \mathbb{V}([\widehat{R}_t(X_0), \widehat{R}_c(X_0)], Y_0) \\ &= \mathcal{O}(\|[\widehat{R}_t, \widehat{R}_c] - [\widehat{R}_t, R_c^*]\|) = \mathcal{O}(\|\widehat{R}_c - R_c^*\|) = \widetilde{\mathcal{O}}(r_c^{1/4} n_s^{-\frac{\tilde{\beta}_c/2}{2\tilde{\beta}_c+1}}). \end{aligned} \quad (\text{B.31})$$

The first equality follows the result (B.7). The second equality follows the definition of the L_2 distance and the last equality follows the result (B.28).

Then we consider the first part of (B.30),

$$\begin{aligned} & \mathbb{V}([R_t^*(X_0), R_c^*(X_0)], Y_0) - \mathbb{V}([\widehat{R}_t(X_0), R_c^*(X_0)], Y_0) \\ & \leq \inf_{\widetilde{R}_t \in \mathcal{F}_{R_t}} |\mathbb{V}([R_t^*(X_0), R_c^*(X_0)], Y_0) - \mathbb{V}([\widetilde{R}_t(X_0), R_c^*(X_0)], Y_0)| \\ & \quad + 2 \sup_{R_t \in \mathcal{F}_{R_t}} |\mathbb{V}_n([R_t(X_0), R_c^*(X_0)], Y_0) - \mathbb{V}([R_t(X_0), R_c^*(X_0)], Y_0)|. \end{aligned}$$

We then bound the approximation error and the stochastic error, respectively. For the approximation error, under Assumption 1-3, we have

$$\begin{aligned} & \mathbb{V}([R_t^*(X_0), R_c^*(X_0)], Y_0) - \mathbb{V}([\widetilde{R}_t(X_0), R_c^*(X_0)], Y_0) \\ & \lesssim \|[R_t^*(X_0), R_c^*(X_0)] - [\widetilde{R}_t(X_0), R_c^*(X_0)]\| \\ & = \|\widetilde{R}_t(X_0) - R_t^*(X_0)\| = \widetilde{\mathcal{O}}(r_t^{1/2} n_0^{-\frac{\widehat{\beta}_t}{2\widehat{\beta}_t+1}}). \end{aligned} \tag{B.32}$$

The result can be derived similar as result (B.16). Then for the stochastic error, we have

$$\sup_{R_t \in \mathcal{F}_{R_t}} |\mathbb{V}_n([R_t(X_0), R_c^*(X_0)], Y_0) - \mathbb{V}([R_t(X_0), R_c^*(X_0)], Y_0)|. \tag{B.33}$$

Similar to (B.22), we have

$$\sup_{R_t \in \mathcal{F}_{R_t}} |\mathbb{V}_n([R_t(X_0), R_c^*(X_0)], Y_0) - \mathbb{V}([R_t(X_0), R_c^*(X_0)], Y_0)| \leq \widetilde{\mathcal{O}}(r_t^{1/2} n_0^{-\frac{\widehat{\beta}_t}{2\widehat{\beta}_t+1}}).$$

Combining these results (B.31), (B.32) and (B.33), we have

$$\begin{aligned} I & = \mathbb{V}([R_t^*(X_0), R_c^*(X_0)], Y_0) - \mathbb{V}([\widehat{R}_t(X_0), R_c^*(X_0)], Y_0) \\ & = \widetilde{\mathcal{O}}(r_t^{1/2} n_0^{-\frac{\widehat{\beta}_t}{2\widehat{\beta}_t+1}}) + \widetilde{\mathcal{O}}(r_c^{1/4} n_s^{-\frac{\widehat{\beta}_c/2}{2\widehat{\beta}_c+1}}). \end{aligned} \tag{B.34}$$

Then we consider the term

$$II = \lambda_C \mathbb{V}(\widehat{R}_t(X_0), \widehat{R}_c(X_0)) - \lambda_C \mathbb{V}(R_t^*(X_0), R_c^*(X_0)).$$

We emphasize that $\widehat{R}_c(\cdot)$ is estimated with the source datasets and thus can be regarded as pre-given regarding the target dataset. Then we consider the following decomposition,

$$\begin{aligned} & \mathbb{V}(\widehat{R}_t(X_0), \widehat{R}_c(X_0)) - \mathbb{V}(R_t^*(X_0), R_c^*(X_0)) \\ & = \mathbb{V}(\widehat{R}_t(X_0), \widehat{R}_c(X_0)) - \mathbb{V}(\widehat{R}_t(X_0), R_c^*(X_0)) \\ & \quad + \mathbb{V}(\widehat{R}_t(X_0), R_c^*(X_0)) - \mathbb{V}(R_t^*(X_0), R_c^*(X_0)). \end{aligned} \tag{B.35}$$

The first term of (B.35) can be bounded as

$$\mathbb{V}(\widehat{R}_t(X_0), \widehat{R}_c(X_0)) - \mathbb{V}(\widehat{R}_t(X_0), R_c^*(X_0)) = \widetilde{\mathcal{O}}(\|\widehat{R}_c(X_0) - R_c^*(X_0)\|) < \widetilde{\mathcal{O}}(r_c^{1/4} n_s^{-\frac{\widehat{\beta}_c}{2\widehat{\beta}_c+1}}).$$

Then we consider the second term of the (B.35),

$$\begin{aligned} & \mathbb{V}(\widehat{R}_t(X_0), R_c^*(X_0)) - \mathbb{V}(R_t^*(X_0), R_c^*(X_0)) \\ & \lesssim \inf_{\widetilde{R}_t \in \mathcal{F}_{R_t}} \left| \mathbb{V}(\widehat{R}_t(X_0), R_c^*(X_0)) - \mathbb{V}(R_t^*(X_0), R_c^*(X_0)) \right| \\ & \quad + 2 \sup_{\widetilde{R}_t \in \mathcal{F}_{R_t}} \left| \mathbb{V}_n(\widehat{R}_t(X_0), R_c^*(X_0)) - \mathbb{V}(\widehat{R}_t(X_0), R_c^*(X_0)) \right|. \end{aligned} \quad (\text{B.36})$$

For the approximation error part, we have

$$\inf_{\widetilde{R}_t \in \mathcal{F}_{R_t}} \left| \mathbb{V}(\widehat{R}_t(X_0), R_c^*(X_0)) - \mathbb{V}(R_t^*(X_0), R_c^*(X_0)) \right| = \widetilde{\mathcal{O}}\left(r_t^{1/2} n_0^{-\frac{\widetilde{\beta}_t}{2\widetilde{\beta}_t+1}}\right). \quad (\text{B.37})$$

For the stochastic error part, we have

$$\sup_{\widetilde{R}_t \in \mathcal{F}_{R_t}} \left| \mathbb{V}_n(\widehat{R}_t(X_0), R_c^*(X_0)) - \mathbb{V}(\widehat{R}_t(X_0), R_c^*(X_0)) \right| = \widetilde{\mathcal{O}}\left(r_t^{1/2} n_0^{-\frac{\widetilde{\beta}_t}{2\widetilde{\beta}_t+1}}\right). \quad (\text{B.38})$$

Combining result (B.37), (B.38), we have

$$II = \widetilde{\mathcal{O}}\left(r_t^{1/2} n_0^{-\frac{\widetilde{\beta}_t}{2\widetilde{\beta}_t+1}}\right) + \widetilde{\mathcal{O}}\left(r_c^{1/4} n_s^{-\frac{\widetilde{\beta}_c/2}{2\widetilde{\beta}_c+1}}\right). \quad (\text{B.39})$$

Then

$$III = \lambda_{E,0} \left[\mathcal{D}(\widehat{R}_t(X_0) || \gamma_{r_t}) - \mathcal{D}(R_t^*(X_0) || \gamma_{r_t}) \right] = \widetilde{\mathcal{O}}\left(r_t^{1/2} n_0^{-\frac{\widetilde{\beta}_t}{2\widetilde{\beta}_t+1}}\right). \quad (\text{B.40})$$

is obtained similarly as the result (B.12), (B.13) and (B.25).

Combining (B.34), (B.39), (B.40), we have the excess risk bound

$$\begin{aligned} & \mathcal{L}_T([\widehat{R}_t, \widehat{R}_c]) - \mathcal{L}_T([R_t^*, R_c^*]) \\ & = I + II + III = \widetilde{\mathcal{O}}\left(r_t^{1/2} n_0^{-\frac{\widetilde{\beta}_t}{2\widetilde{\beta}_t+1}}\right) + \widetilde{\mathcal{O}}\left(r_c^{1/4} n_s^{-\frac{\widetilde{\beta}_c/2}{2\widetilde{\beta}_c+1}}\right). \end{aligned}$$

The proof is completed.

C Additional simulation results

C.1 Details for TransIRM

TransIRM is based on the invariant risk minimization (IRM) (Arjovsky et al., 2019) which aims to learn the predictive representation $R_{so}(X)$ from source domains.

In this paper, we use IRMv1 (Arjovsky et al., 2019). The objective function in source domains is

$$\mathcal{L}_S^{IRM}(w, g_c, R_{so}) = \sum_{s=1}^S \left[\mathcal{L}_{pred}(w^T g_c \circ R_{so}(X_s), Y_s) + \lambda \|\nabla_{w|w=1} \mathcal{L}_{pred}(w^T g_c \circ R_{so}(X_s), Y_s)\|_2^2 \right],$$

where \mathcal{L}_{pred} is the mean square loss for regression and cross-entropy loss for classification, g_c is the regression function with the representation as input. After training, we only transfer the representation R_{so} to the target domain. The objective function of TransIRM in the target domain is defined as

$$\mathcal{L}_{pred}(g_0 \circ R_{so}(X_0), Y_0),$$

where R_{so} is frozen and g_0 is the prediction function taking R_{so} as input.

The $R_{so}(X)$ learned with TransIRM contains useful information for predicting on the source domain but lacks sufficiency guarantees. We consider TransIRM as a competitor of the proposed method to illustrate the importance of adapting to the specific characteristics of the target domain.

C.2 Details of implementation

In this part we give the details of the network structure in all the numerical experiments. We give the network structure of the 4 methods in the simulation in the Figure S8- S11.

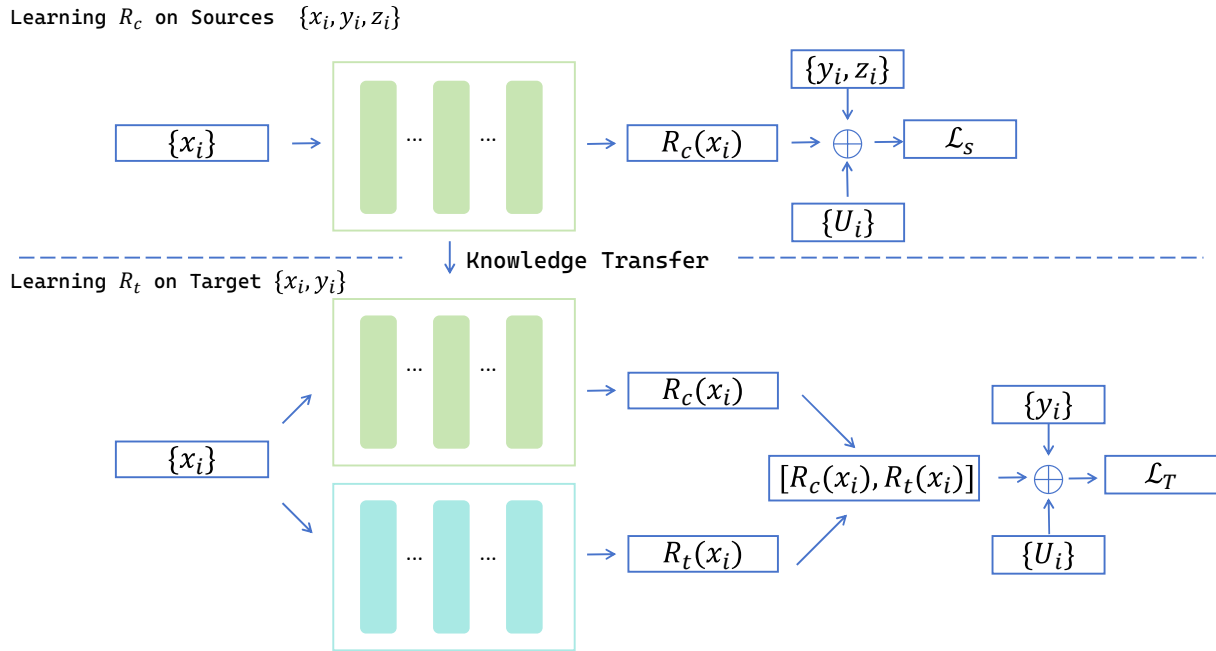


Figure S8: The Structure of the TESR framework

The hyper-parameters for the simulated experiments are given in Table S4, where λ_E , λ_Z , λ_C , $\lambda_{E,0}$ are parameters in the objective functions, bs is the mini-batch size, ld is the dimension of representation and loop indicates the number of times to repeat the experiments. In the simulation, we consider the RMSprop algorithm for the optimization for the neural network with the PyTorch package for implementation.

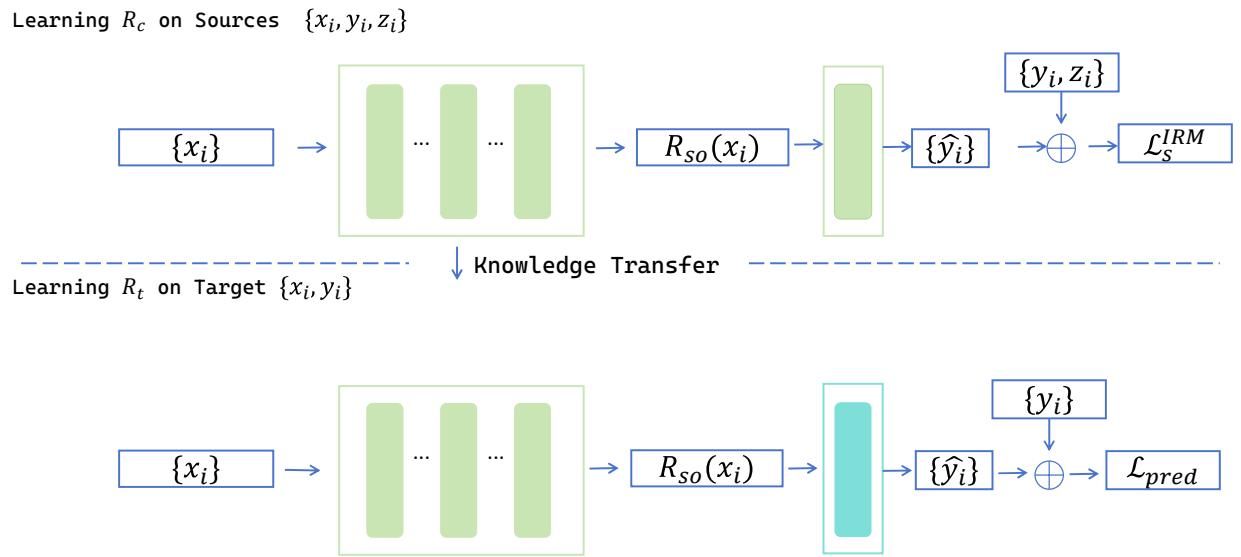


Figure S9: The Structure of the TransIRM framework. TransIRM is an end-to-end method and the prediction model taken the representation as inputs are shown in the figure.

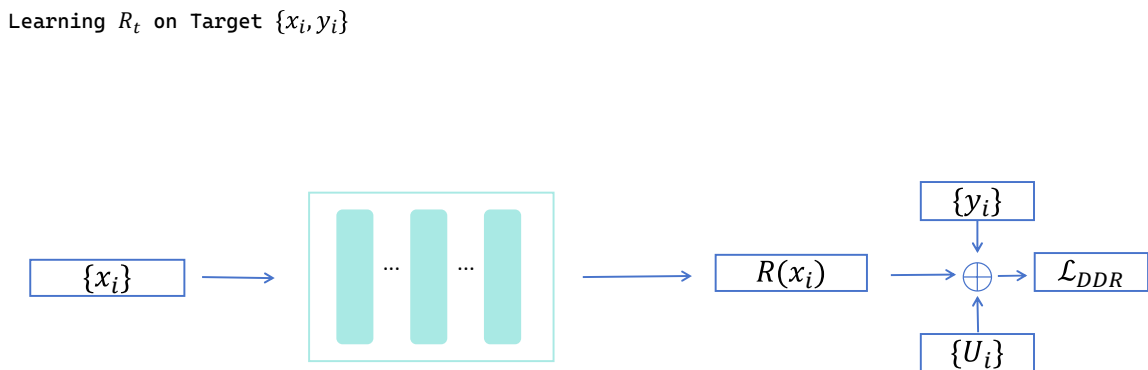


Figure S10: The Structure of the DDR framework

Learning R_t on Target $\{x_i, y_i\}$

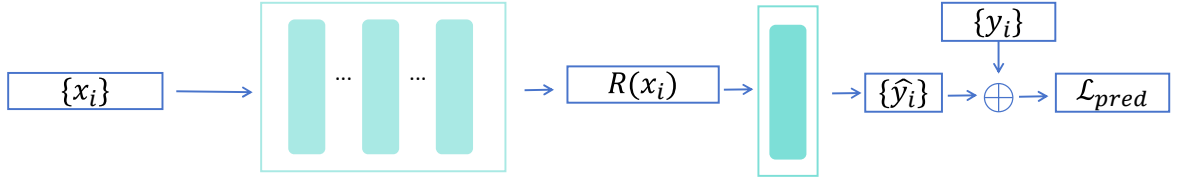


Figure S11: The Structure of the DNN framework.

Table S4: Hyper-parameters for TESR in simulated examples.

	λ_E	λ_Z	λ_C	$\lambda_{E,0}$	bs	ld	Learning rate	weight decay	Epoch
Example 1	0.1	0.1	0.1	0.1	64	32	1e-3	1e-4	300
Example 2	0.1	0.1	0.1	0.1	64	32	1e-3	1e-4	300
Example 3	0.1	0.1	0.1	0.1	64	32	1e-3	1e-4	300

Table S5: Hyper-parameters for TESR in Real data cases.

	λ_E	λ_Z	λ_C	$\lambda_{E,0}$	bs	ld	Learning rate	weight decay	Epoch
PACS	0.01	0.01	1	0.01	128	64	$0.5 \times 1e-3$	1e-4	300
JAM2	0.01	0.01	0.1	0.01	64	64	$0.5 \times 1e-3$	1e-4	200

Table S6: MLP architectures for R_c and R_t in simulation examples. The d in the input size is the dimension of X .

Layers	Details	R_c			R_t	
		Input size	Output size		Input size	Output size
Layer 1	Linear	d	64	Linear	d	64
Activation	LeakyReLU(0.2)	64	64	LeakyReLU(0.2)	64	64
Layer 2	Linear	64	32	Linear	64	32
Activation	LeakyReLU(0.2)	32	32	LeakyReLU(0.2)	32	32
Layer 3	Linear	32	32	Linear	32	32

Table S7: CNN architectures for the analysis on dataset PACS. The BN denotes batch normalization layer.

		R_c		R_t		
Layers	Details	Input size	Output size	Details	Input size	Output size
Layer 1	Convolution 3x3, BN	(3,32,32)	(48,32,32)	Convolution 3x3, BN	(3,32,32)	(48,32,32)
Activation	LeakyReLU(0.2)	(48,32,32)	(48,32,32)	LeakyReLU(0.2)	(48,32,32)	(48,32,32)
Layer 2	Convolution 3x3, BN	(48,32,32)	(96,32,32)	Convolution 3x3, BN	(48,32,32)	(96,32,32)
Activation	LeakyReLU(0.2)	(96,32,32)	(96,32,32)	LeakyReLU(0.2)	(96,32,32)	(96,32,32)
Layer 3	MaxPooling 2x2	(96,32,32)	(96,16,16)	MaxPooling 2x2	(96,32,32)	(96,16,16)
Layer 4	Convolution 3x3, BN	(96,16,16)	(192,16,16)	Convolution 3x3, BN	(96,16,16)	(192,16,16)
Activation	LeakyReLU(0.2)	(192,16,16)	(192,16,16)	LeakyReLU(0.2)	(192,16,16)	(192,16,16)
Layer 5	Convolution 3x3, BN	(192,16,16)6	(256,16,16)	Convolution 3x3, BN	(192,16,16)	(256,16,16)
Activation	LeakyReLU(0.2)	(256,16,16)	(256,16,16)	LeakyReLU(0.2)	(256,16,16)	(256,16,16)
Layer 6	MaxPooling 2x2	(256,16,16)	(256,8,8)	MaxPooling 2x2	(256,16,16)	(256,8,8)
Layer 7	Linear	16384	1024	Linear	16384	1024

Table S8: MLP architectures for R_c and R_t in the real data analysis for Gene JAM2.

		R_c		R_t		
Layers	Details	Input size	Output size	Details	Input size	Output size
Layer 1	Linear	1813	64	Linear	1813	64
Activation	LeakyReLU(0.2)	64	64	LeakyReLU(0.2)	64	64
Layer 2	Linear	64	64	Linear	64	64
Activation	LeakyReLU(0.2)	64	64	LeakyReLU(0.2)	64	64
Layer 3	Linear	64	64	Linear	64	64

C.3 Additional simulation results

C.3.1 Additional simulation: knowledge transfer from regression to regression tasks

In this part, we give additional simulation results where the sources task $\mathcal{D}_{s,s} = 1, 2, 3, 4$ and the target task \mathcal{D}_0 are all regression tasks. In other word, the response in all the tasks are all continuous variable. This is a commonly considered scenario in conventional transfer learning methods.

In this example, the response on the target domain \mathcal{D}_0 is continuous and the L_2 loss is considered for the prediction modules of all four methods. This is different from the main text, where the logistic loss is applied to estimate the binary responses in the target domains.

Example S.1 We generate 4 sources and 1 target datasets with the following model:

- $\mathcal{D}_0 : y = 3f_1(x_1) + 1.5f_2(x_2)f_3(x_3) + f_6(x_6) + \epsilon_0;$

and the sources models:

- $\mathcal{D}_1 : y = 2f_1(x_1) + 1f_2(x_2)f_3(x_3) + f_4(x_4) + \epsilon_1;$
- $\mathcal{D}_2 : y = 2f_1(x_1) + 1f_2(x_2)f_3(x_3) + 2f_4(x_4) + \epsilon_2;$
- $\mathcal{D}_3 : y = 2f_1(x_1) + 1.5f_2(x_2)f_3(x_3) + f_5(x_5) + \epsilon_3;$
- $\mathcal{D}_4 : y = 2f_1(x_1) + 1.5f_2(x_2)f_3(x_3) + 2f_5(x_5) + \epsilon_4;$

where $f_1(u) = u$, $f_2(u) = 2u + 1$, $f_3(u) = 2u - 1$, $f_4(u) = 0.1 \sin(\pi u) + 0.2 \cos(\pi u)$, $f_5(u) = \sin(\pi u)/(2 - \sin(\pi u))$, $f_6(u) = u(|u| + 1)^2$. The $x \sim U(0, 1)$ follows the uniform distribution and ϵ_s for $s = 0, 1, 2, 3, 4$ are independent random variables drawn from $N(0, 0.5^2)$.

In Example S.1, we study the numerical performance with different (n_s, n_0, p) . As shown in Figure S12, the proposed TESR method outperforms all its competitor. It also shows the superiority and applicability of the proposed method.

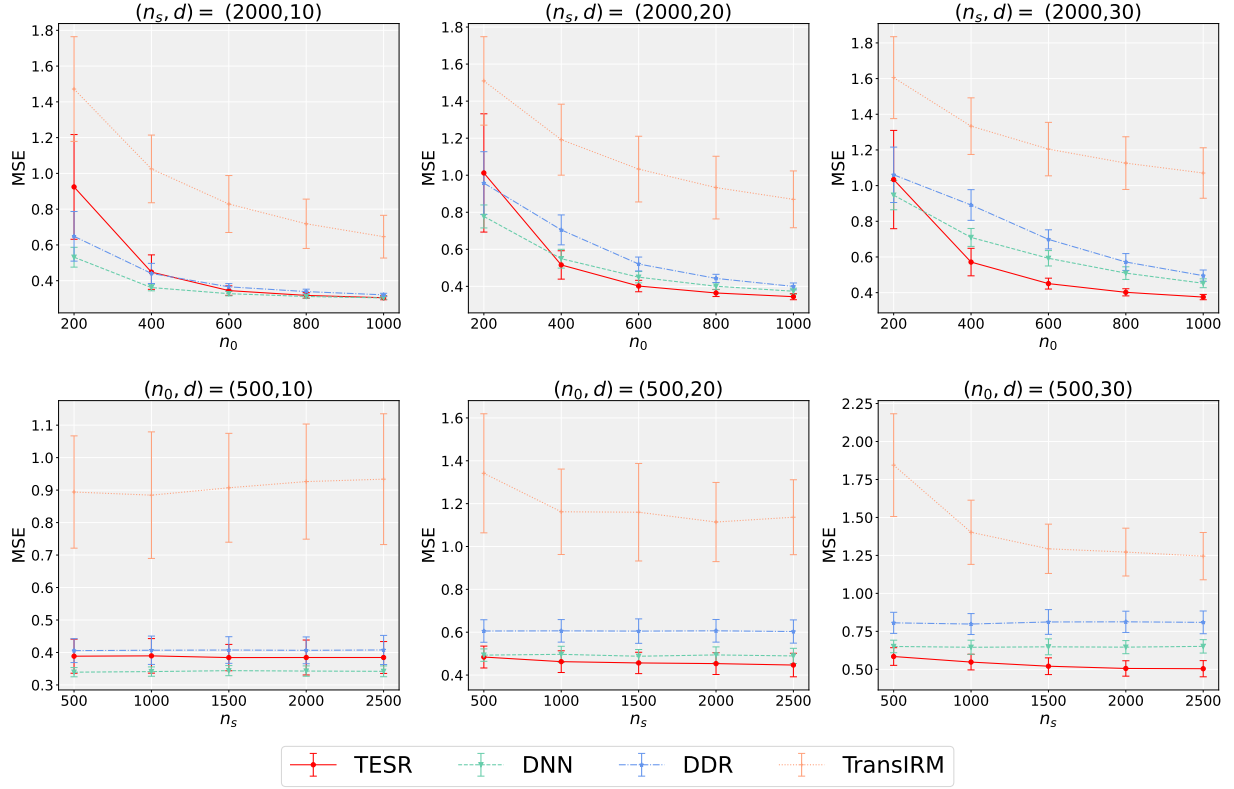


Figure S12: the MSE on the \mathcal{D}_0 in Example S.1 with different (n_s, n_0, d) .

C.3.2 Distance between the sources and the target in Example 3

In Example 3, we consider two types of model departures. In Figure S13, we calculate the numerical L_1 distance and the cosine distance under these departures.

Specifically, for two regression function $g_1(x)$, $g_2(x)$, the L_1 distance is defined as

$$\int |g_1(x) - g_2(x)| dP(x),$$

and the cosine distance is defined as

$$1 - Cor \left[g_1(x), g_2(x) \right].$$

It is clear that cosine distance lies in $[0, 1)$ implying the positive correlation and $(1, 2]$ for negative correlation.

In the left panel of Figure S13, we report the L_1 distance under the Type I departure. It is clear that L_1 distance increases with $s = 1, \dots, 6$. We note that the $\mathcal{D}_1, \dots, \mathcal{D}_6$ have larger L_1 distance with the target data, compared with the $\mathcal{D}_7, \mathcal{D}_8$. However, $\mathcal{D}_7, \mathcal{D}_8$ contain no useful information for the target task. It implies the invalidity of L_1 distance as an task similarity measure.

In the right panel of Figure S13, we report the cosine similarity distances under the Type II departure. It is clear that correlation changes for $s = 1, \dots, 6$. We note that the correlation between the target task and $\mathcal{D}_1, \dots, \mathcal{D}_6$ can be positive and negative. It introduces more heterogeneity for the transfer learning problem.

The experiment results in Example 3 support our argument that TESR does not rely on the the premise of the regression function similarity between the source and the target data.

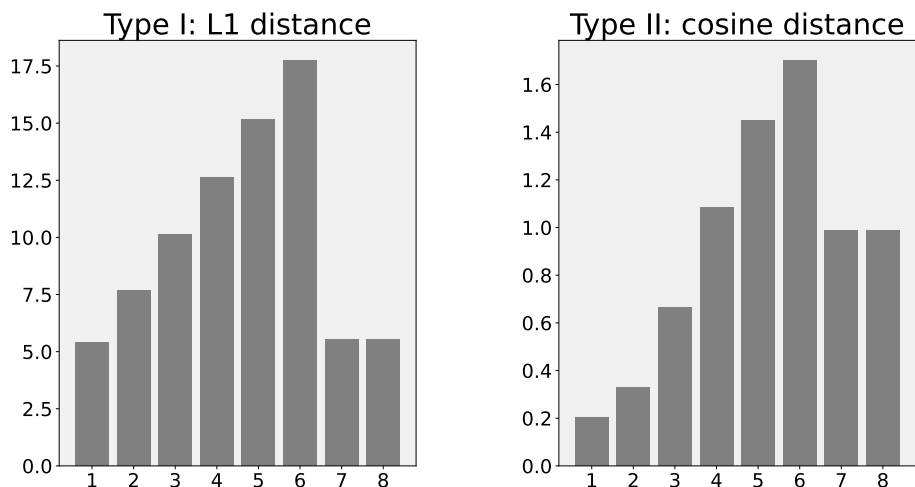


Figure S13: The empirical distances between the regression functions from the sources and the target in Example 3.